

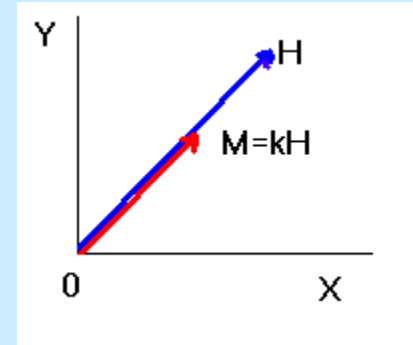
ANISOTROPY OF MAGNETIC SUSCEPTIBILITY

Magnetization of Isotropic Substance

$$M_1 = k H_1$$

$$M_2 = k H_2$$

$$M_3 = k H_3$$



Magnetization of Anisotropic, Linearly Magnetic Substance

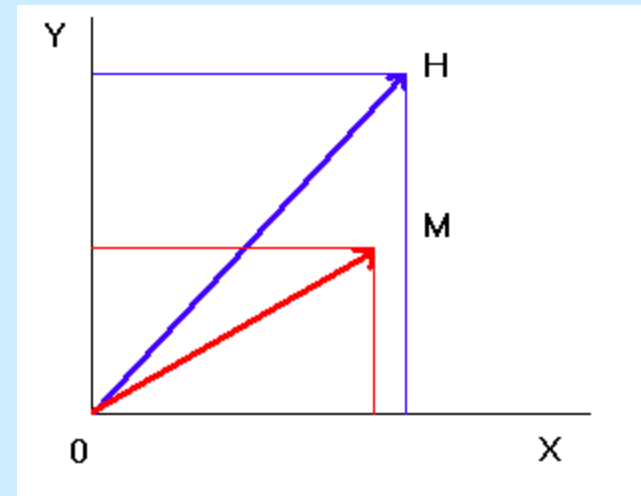
$$M_1 = k_{11} H_1 + k_{12} H_2 + k_{13} H_3$$

$$M_2 = k_{21} H_1 + k_{22} H_2 + k_{23} H_3$$

$$M_3 = k_{31} H_1 + k_{32} H_2 + k_{33} H_3$$

In Matrix Notation

$$\begin{vmatrix} M_1 \\ M_2 \\ M_3 \end{vmatrix} = \begin{vmatrix} k_{11} & k_{12} & k_{13} \\ k_{21} & k_{22} & k_{23} \\ k_{31} & k_{32} & k_{33} \end{vmatrix} \begin{vmatrix} H_1 \\ H_2 \\ H_3 \end{vmatrix}$$



Magnetization Vector, Susceptibility Tensor, Field Intensity Vector

Principal Susceptibilities, Principal Directions

$$M_1 = k_{11} H_1 + k_{12} H_2 + k_{13} H_3$$

$$M_2 = k_{21} H_1 + k_{22} H_2 + k_{23} H_3$$

$$M_3 = k_{31} H_1 + k_{32} H_2 + k_{33} H_3$$

For each tensor such a coordinate system exists where

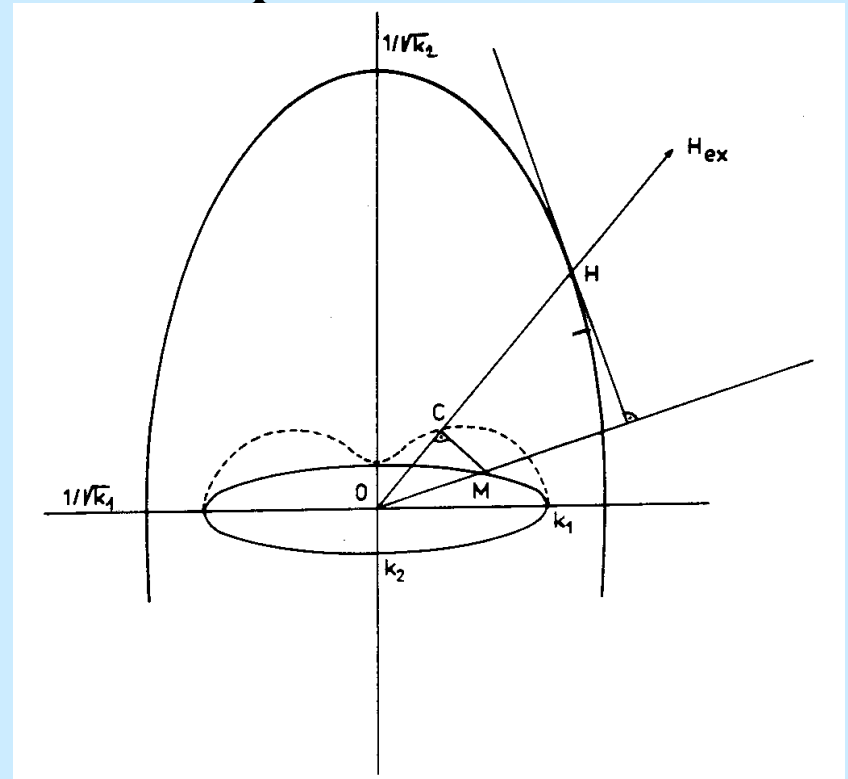
$$M_1 = k_{11} H_1$$

$$M_2 = k_{22} H_2$$

$$M_3 = k_{33} H_3$$

Axes of this system are parallel to the susceptibility ellipsoid axes, in which magnetization is parallel to the field.

Susceptibilities along ellipsoid axes are **Principal Susceptibilities**
Directions of ellipsoid axes are **Principal Directions**



AMS Parameters and Plots

$$P = k_1/k_3$$

degree of AMS

$$k_1 \geq k_2 \geq k_3$$

$$L = k_1/k_2$$

magnetic lineation

$$F = k_2/k_3$$

magnetic foliation

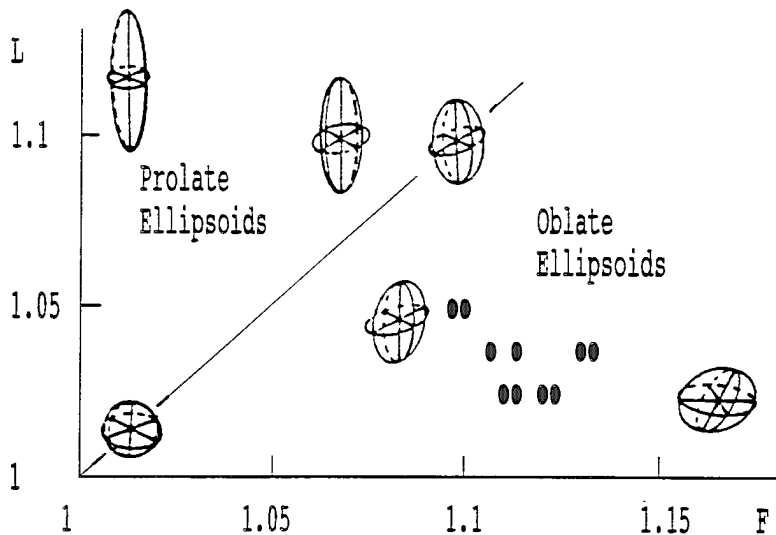
$$n_1 = \ln k_1, n_2 = \ln k_2,$$

$$T = (2n_2 - n_1 - n_3)/(n_1 - n_3)$$

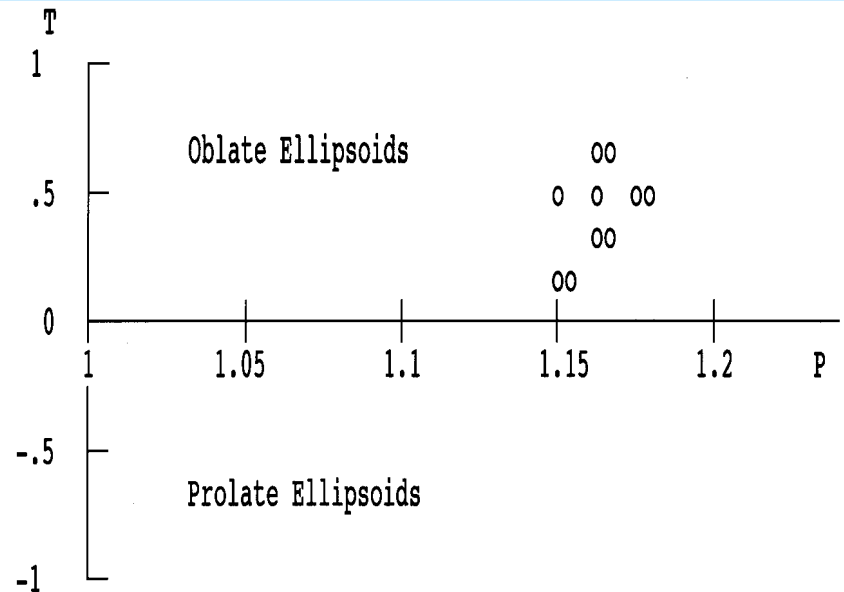
shape parameter

$$n_3 = \ln k_3$$

Flinn Type Plot

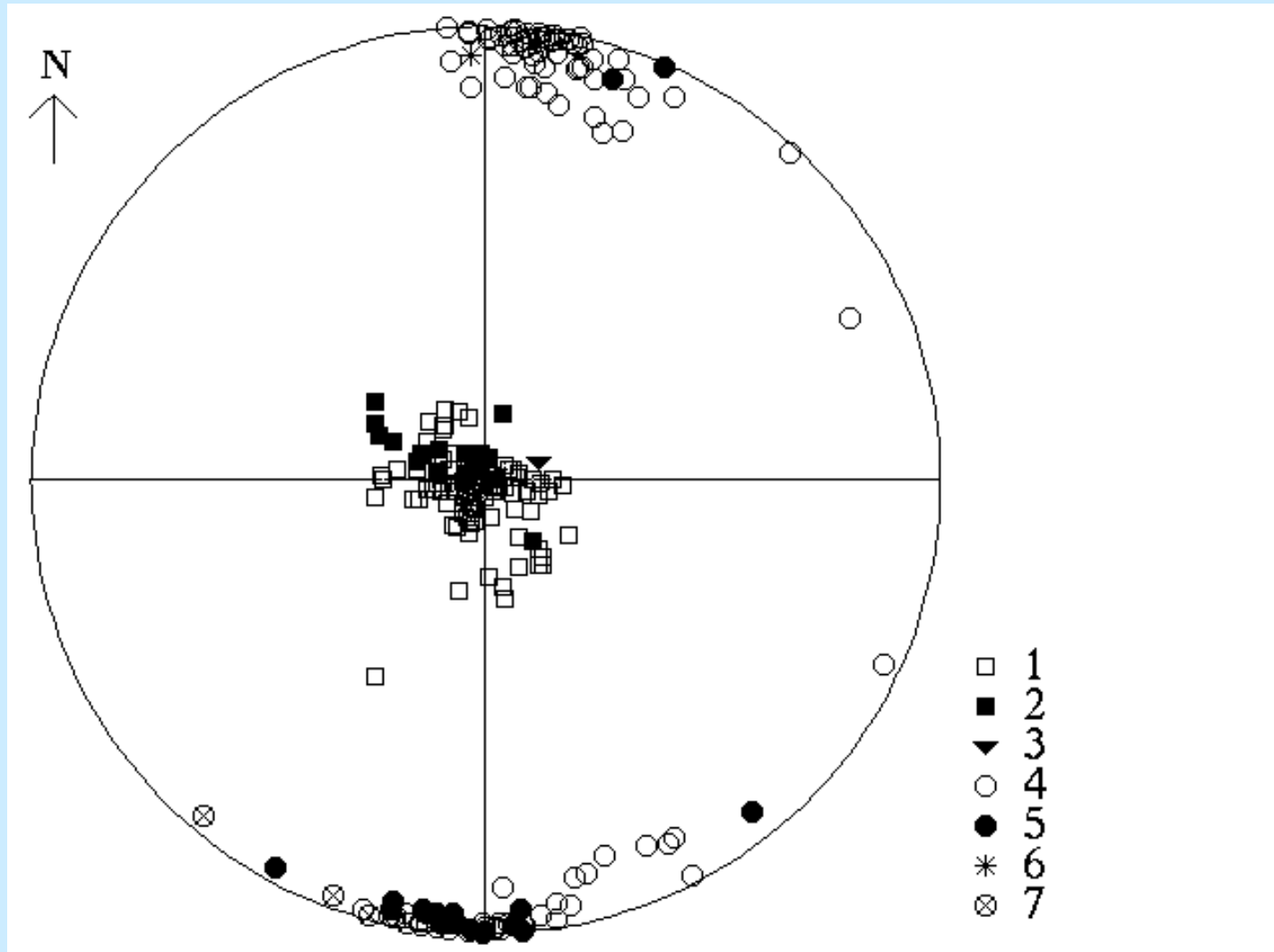


Jelinek Type Plot

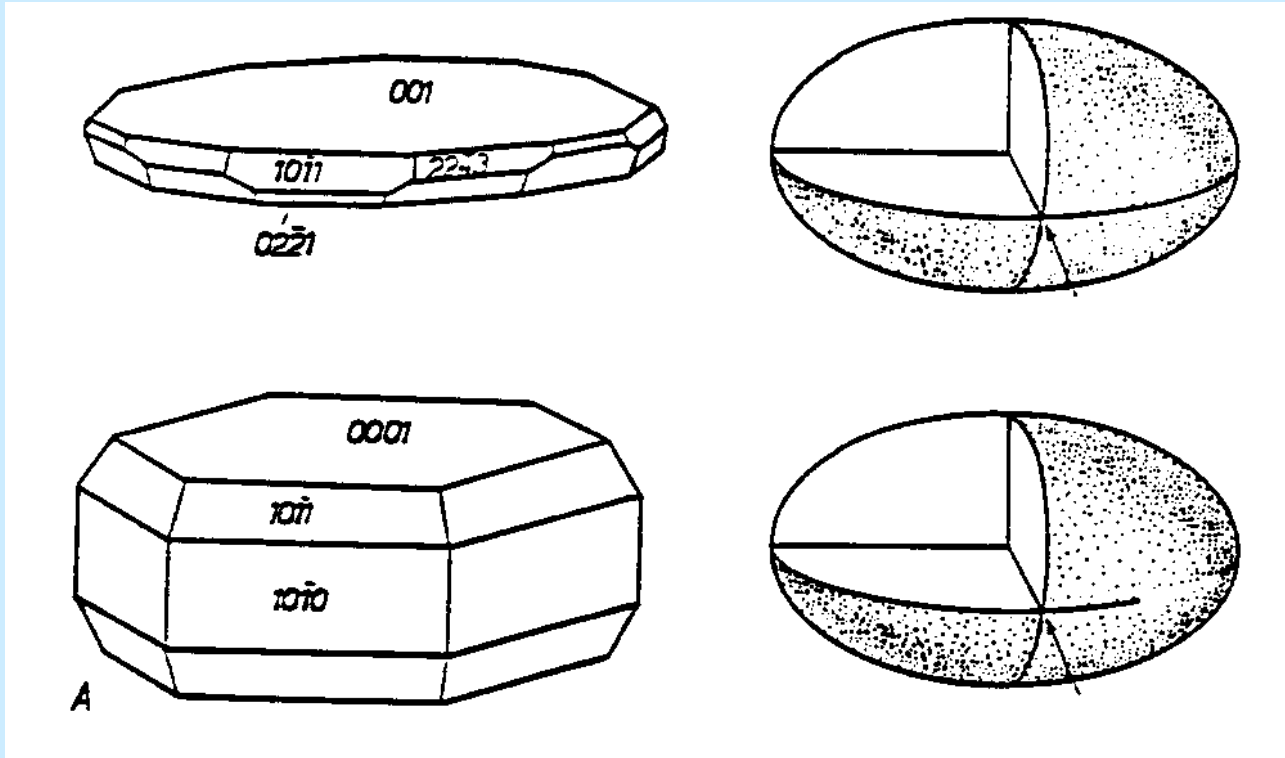


ORIENTATIONS OF MAGNETIC FABRIC ELEMENTS

equal-area projection on lower hemisphere



AMS of Minerals 1



Hematite

$$k_1 = k_2 \gg k_3$$

$$P > 100$$

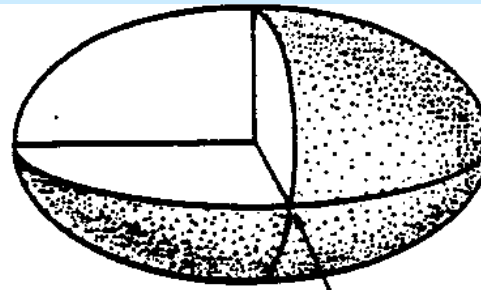
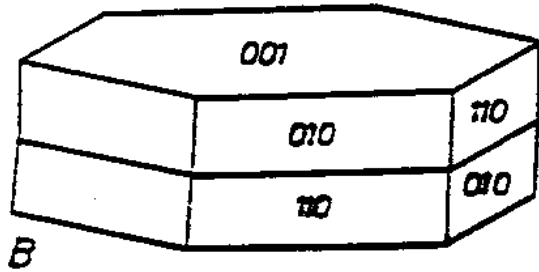
Pyrrhotite

$$k_1 = k_2 \gg k_3$$

$$P > 300$$

Grain AMS is due to the crystal lattice (magnetocrystalline AMS)

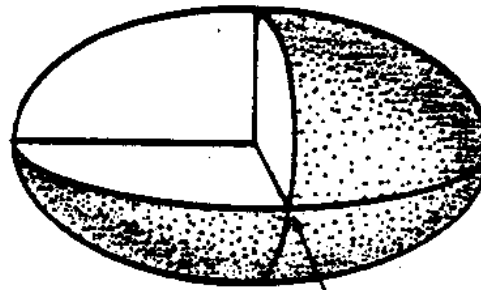
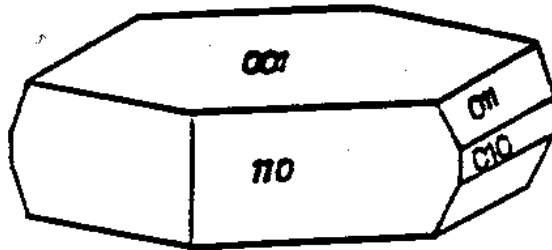
AMS of Minerals 2



Biotite

$$k_1 = k_2 > k_3$$

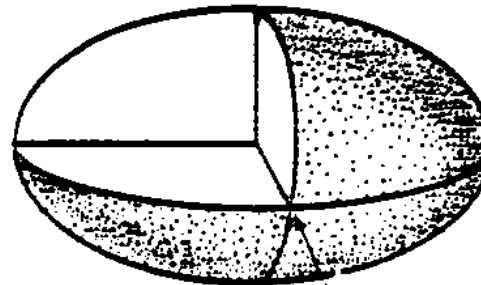
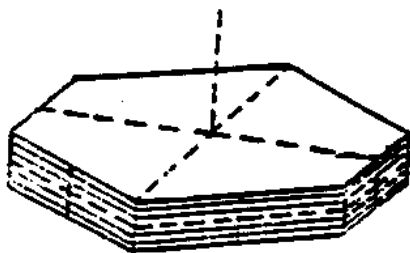
$$P = 1.2-1.6$$



Muscovite

$$k_1 = k_2 > k_3$$

$$P = 1.3-1.4$$



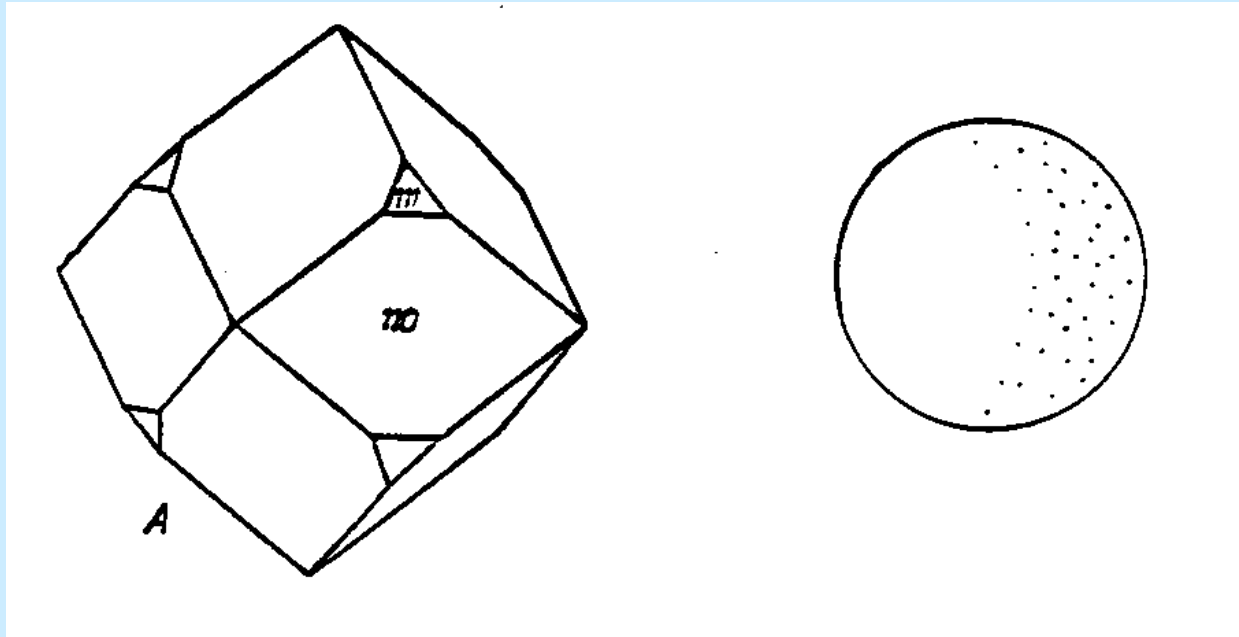
Chlorite

$$k_1 = k_2 > k_3$$

$$P = 1.2-1.8$$

Grain AMS is due to the crystal lattice (magnetocrystalline AMS)

AMS of Minerals 4



Magnetite is internally isotropic in weak field.

$$P = (1 + \kappa N_c) / (1 + \kappa N_a)$$

$$P = 1.1 - 3.0$$

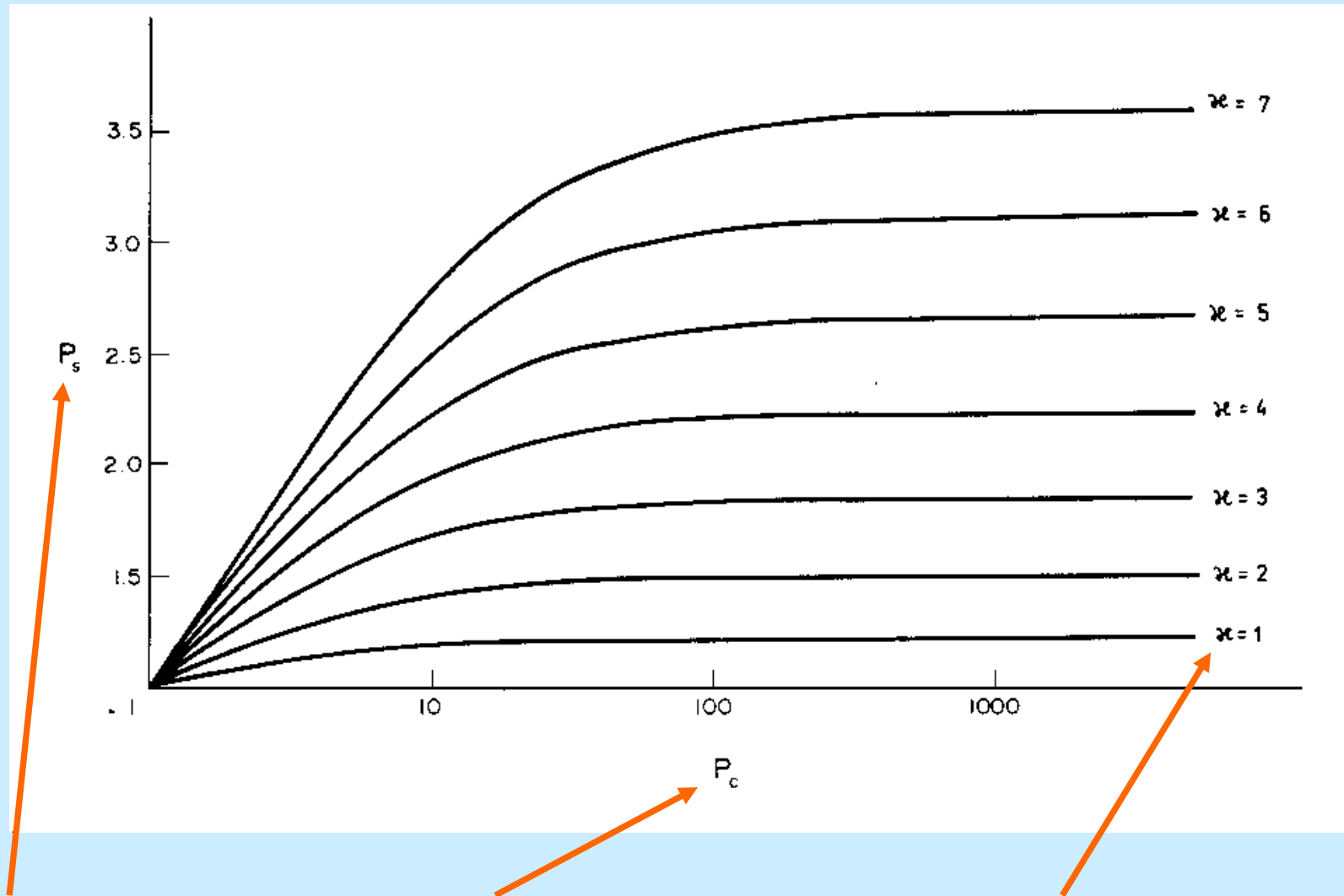
κ – intrinsic susceptibility

N – demagnetizing factor

(controlled by grain shape)

Grain AMS is due to the grain shape (shape AMS)

Effects of Grain AMS and Preferred Orientation: a model



Rock degree of AMS, Grain degree of AMS, Concentration Parameter

AMS OF SEDIMENTARY ROCKS

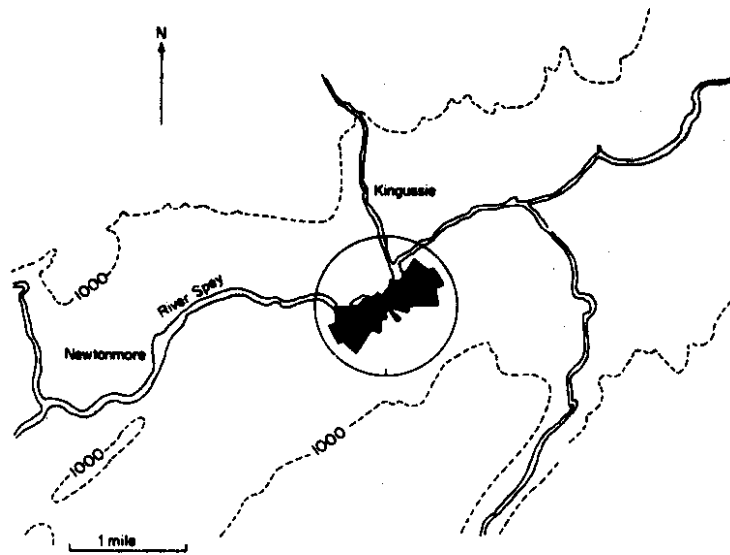


Fig. 5. Parallelism of magnetic lineation direction with channel axis, fluvio-glacial sediments, Kingussie, Scotland. After Hamilton and Rees (1970). Courtesy of Academic Press Ltd.

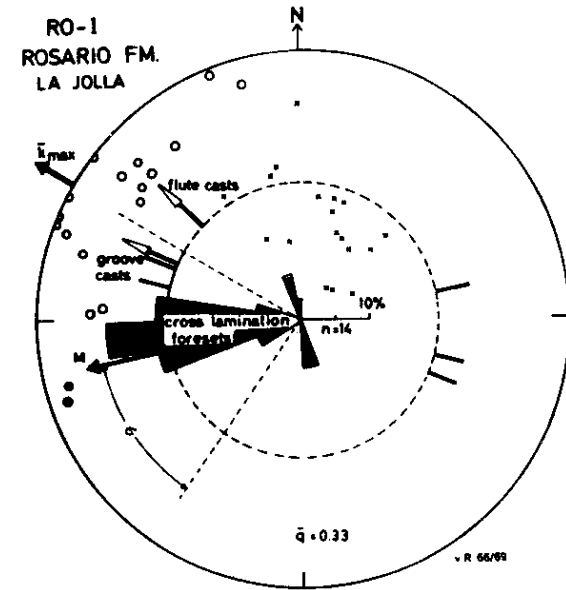
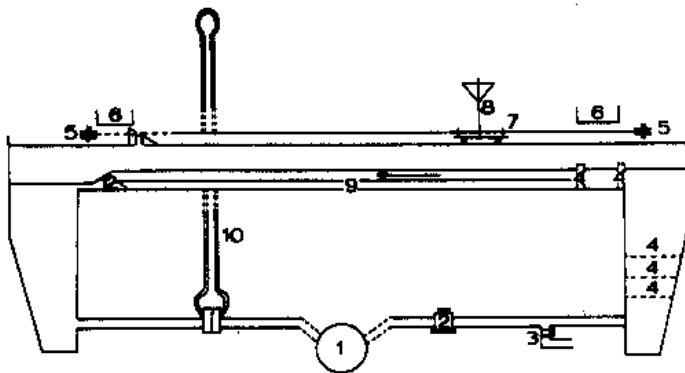


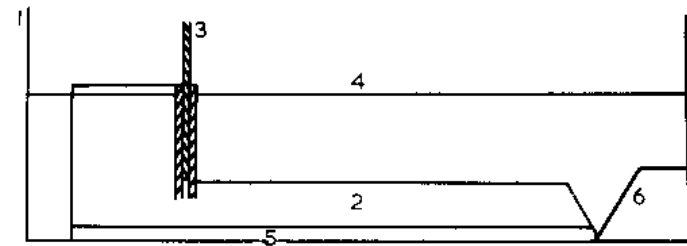
Fig. 6. Comparison of magnetic and sedimentary fabric, Rosario Formation, La Jolla, California. Crosses: minimum susceptibility directions, open circles: maximum susceptibility directions. Equal area projection on lower hemisphere (projection plane = bedding plane). Adapted from von Rad (1971). Courtesy of the author.

Flume Depositions



- | | | |
|----------------------|----------------------|-----------------------------|
| 1. Centrifugal pump. | 5. Pulleys. | 9. Sediment bed. |
| 2. Flow-rate valve. | 6. Collecting boxes. | 10. Differential Monometer. |
| 3. Outflow tap. | 7. Messenger. | 11. Messenger release |
| 4. Baffle plate. | 8. Sand Hopper. | 12. Weir. (mechanism). |

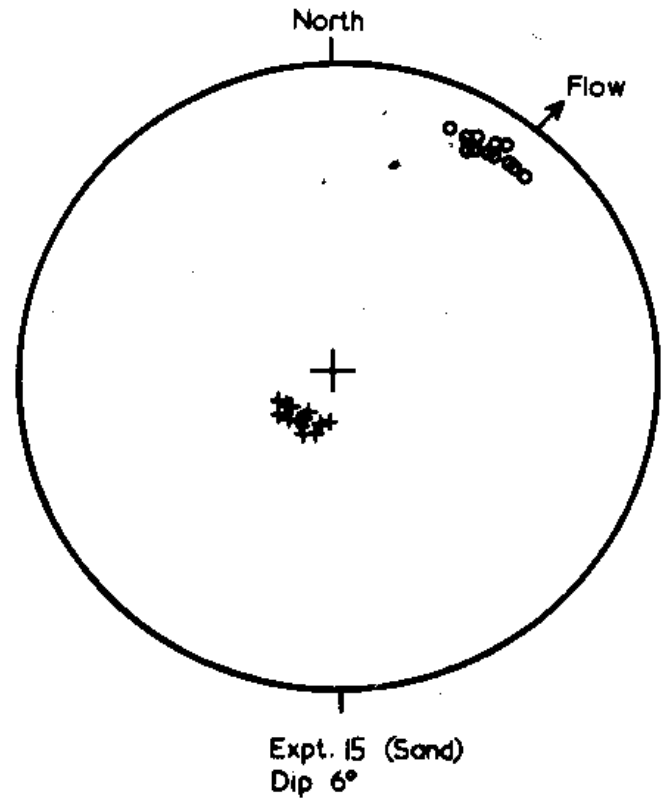
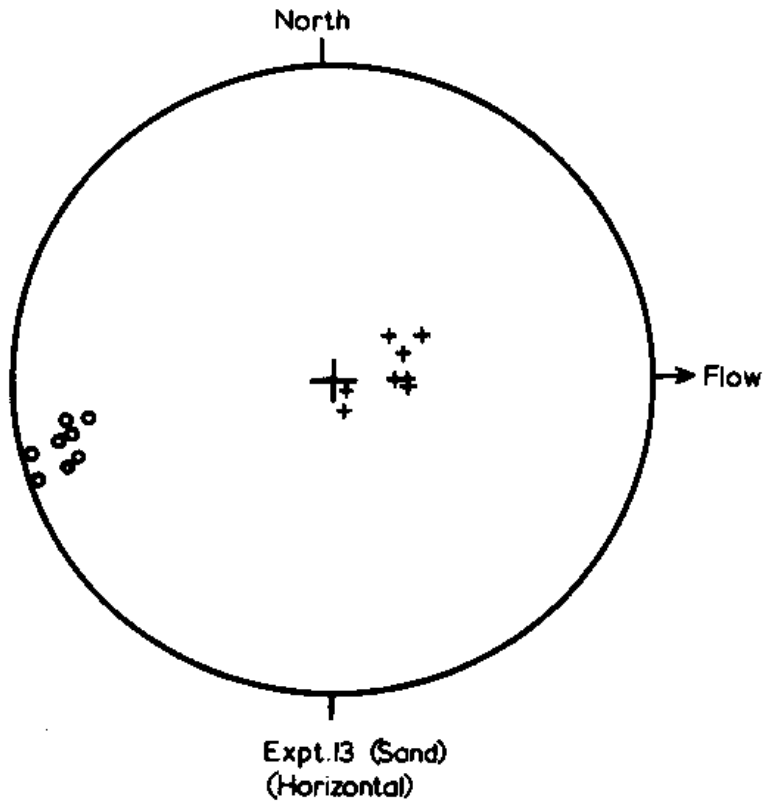
Fig. 1. Recirculating flume used for the depositions from running water (experiments 1–6).



- | | |
|------------------|---------------------------|
| 1. Plastic bath. | 4. Water level. |
| 2. Channel. | 5. Sediment deposit. |
| 3. Sliding trap. | 6. Perforated zinc sheet. |

Fig. 2. Apparatus used for the density current depositions (experiments 13–16).

Experiments 13,15

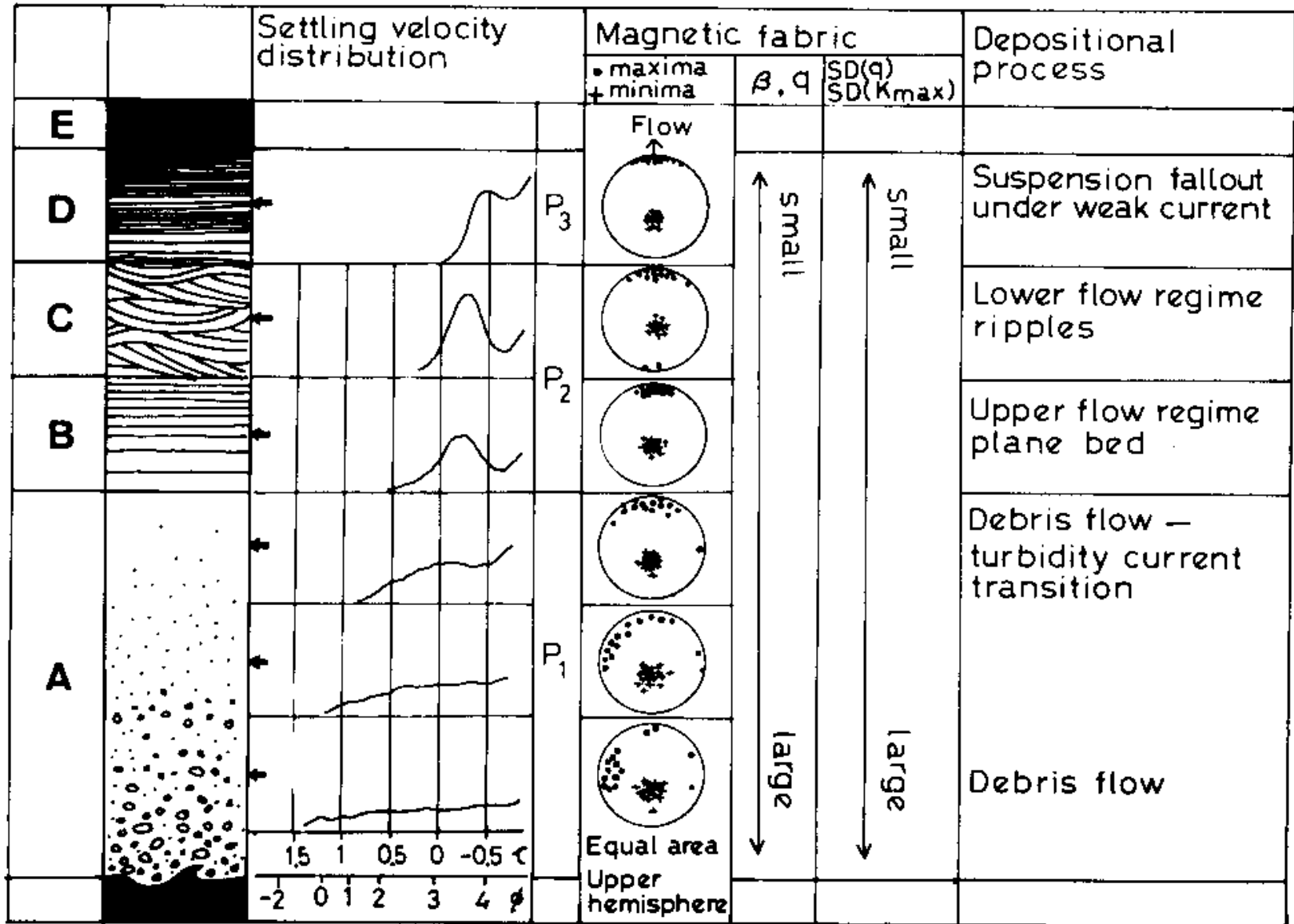


density current, flat bed N/A

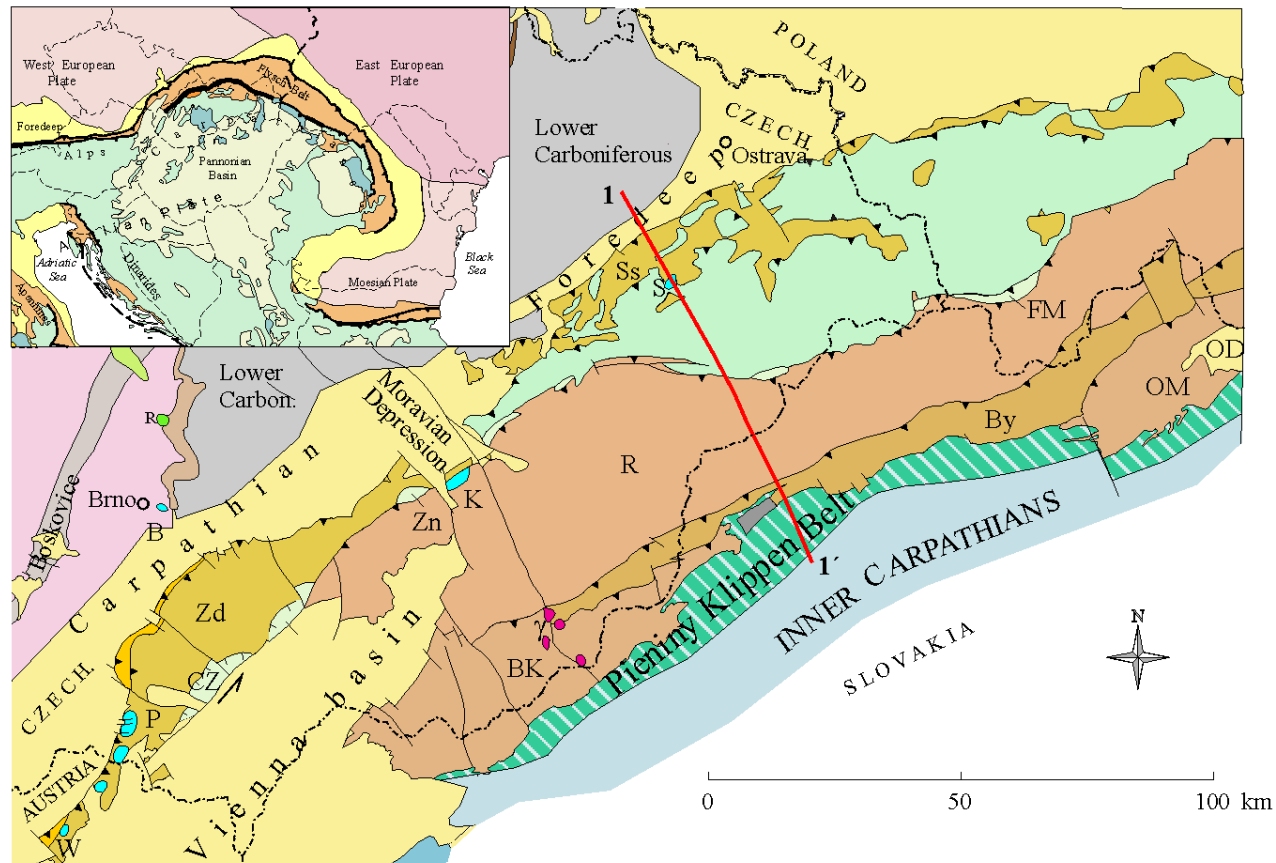
density current, flat bed

AMS in Turbidites





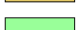

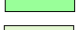


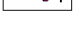
e
f
e
1



Flysch Belt of West Carpathians – geol. scheme

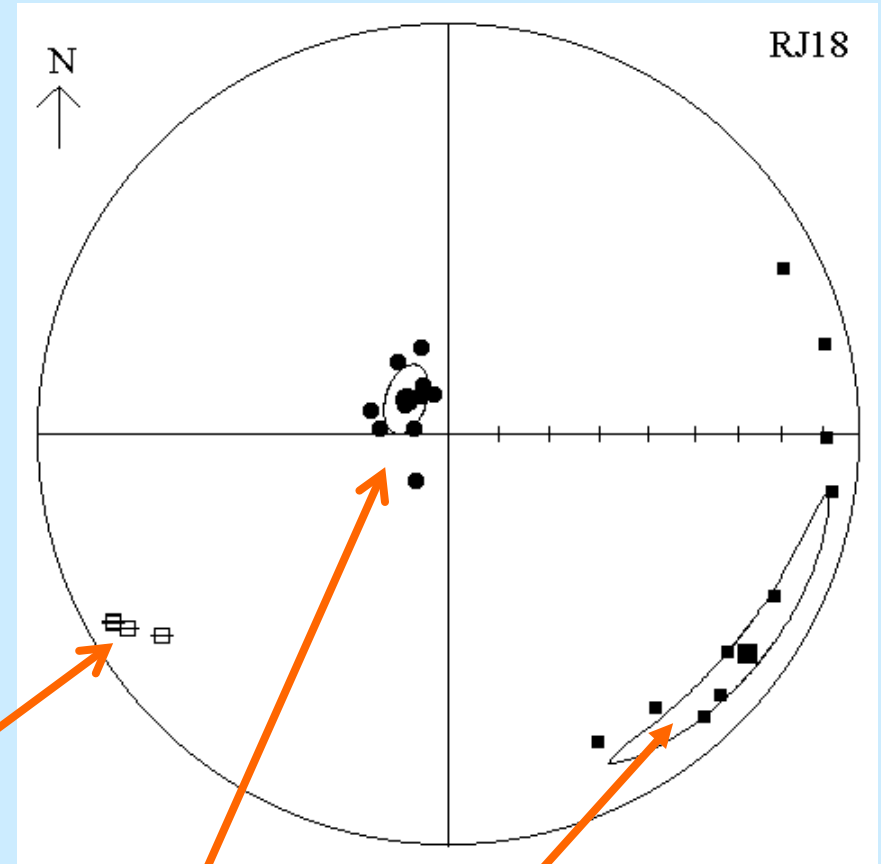
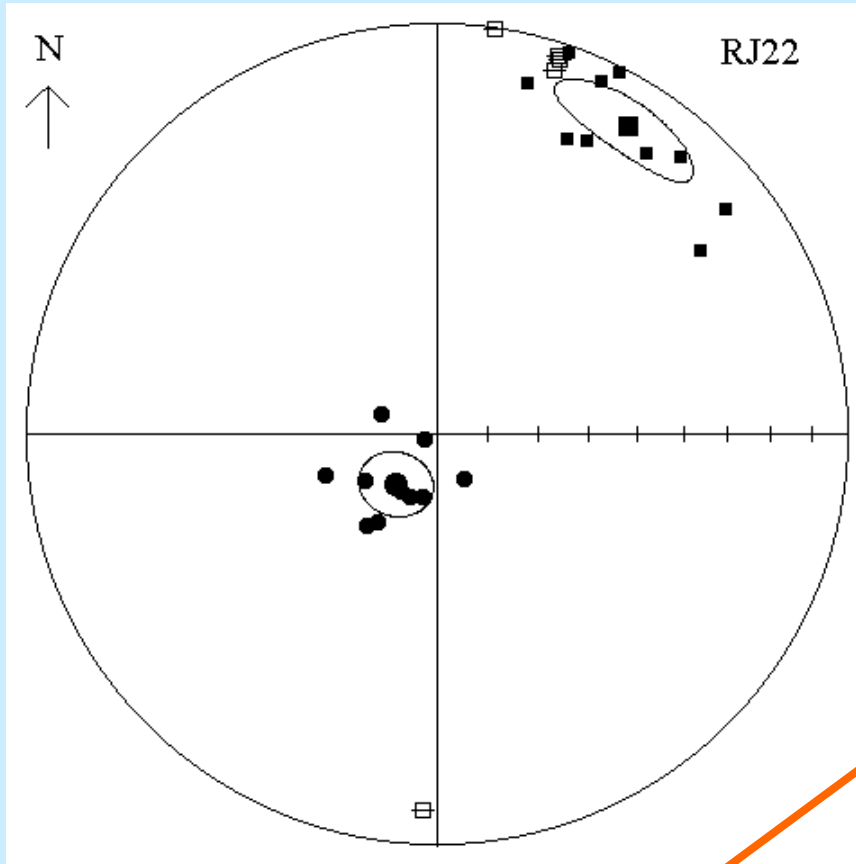


LEGEND

- | | | | |
|---|--|---|---|
|  | Pouzdrany Unit |  | Bystrica Unit (By) |
|  | Waschberg (W), Zdanice (Zd) and Subsilesian (Ss) units |  | Bile Karpaty (BK) and Oravská Magura (OM) |
|  | Silesian Unit |  | Jurassic Limestone (P-Pavlov, K-Kurovice, S-Štramberk, L-Lukoveček, B-Brno) |
|  | Foremagura (FM), Zdonky (Zn), and Cejc-Zajeci (CZ) units |  | Tertiary volcanics |
|  | Raca Unit (R) |  | OD Orava depression |

Flysch Belt of West Carpathians - orientations

bedding corrected for tilt



current direction

MF pole

ML

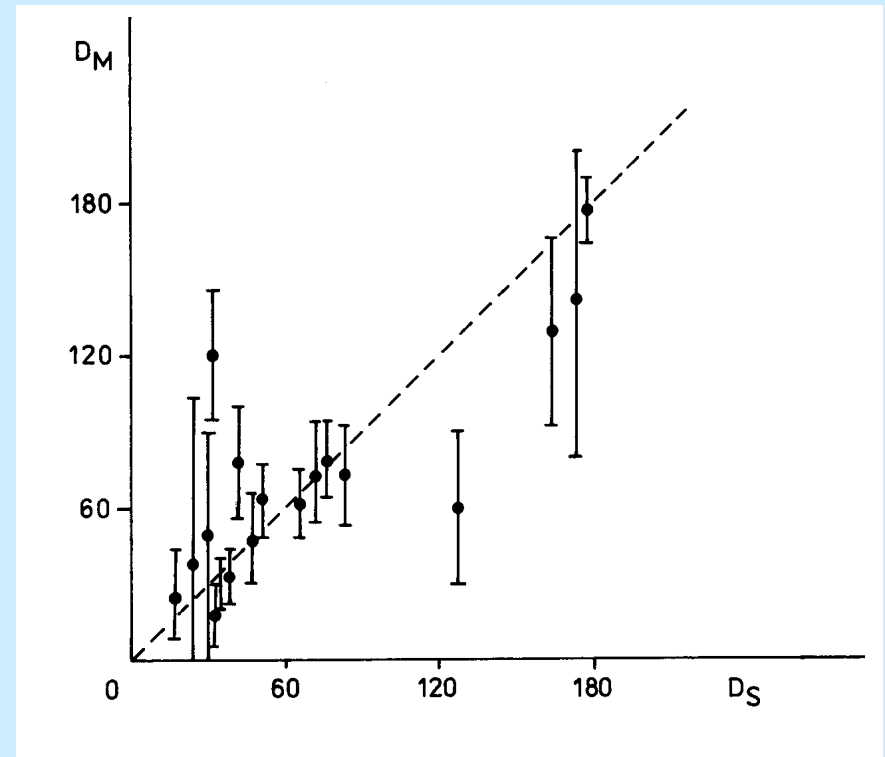
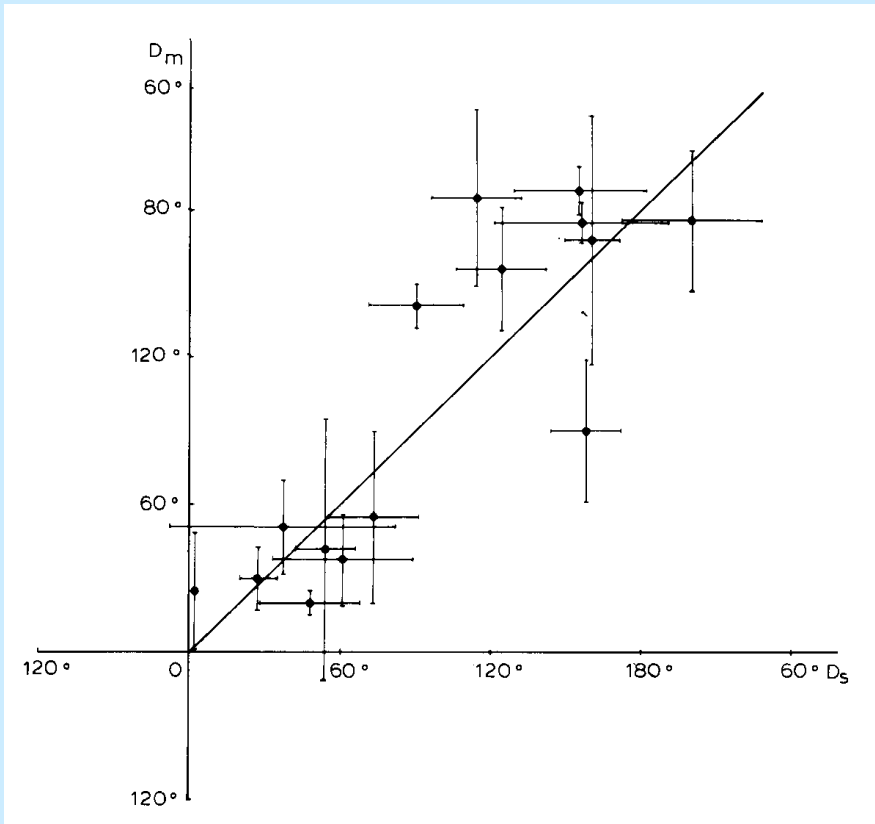
ML parallel to current direction

ML perpendicular to current direction

Magnetic vs. Sedimentary Lineations

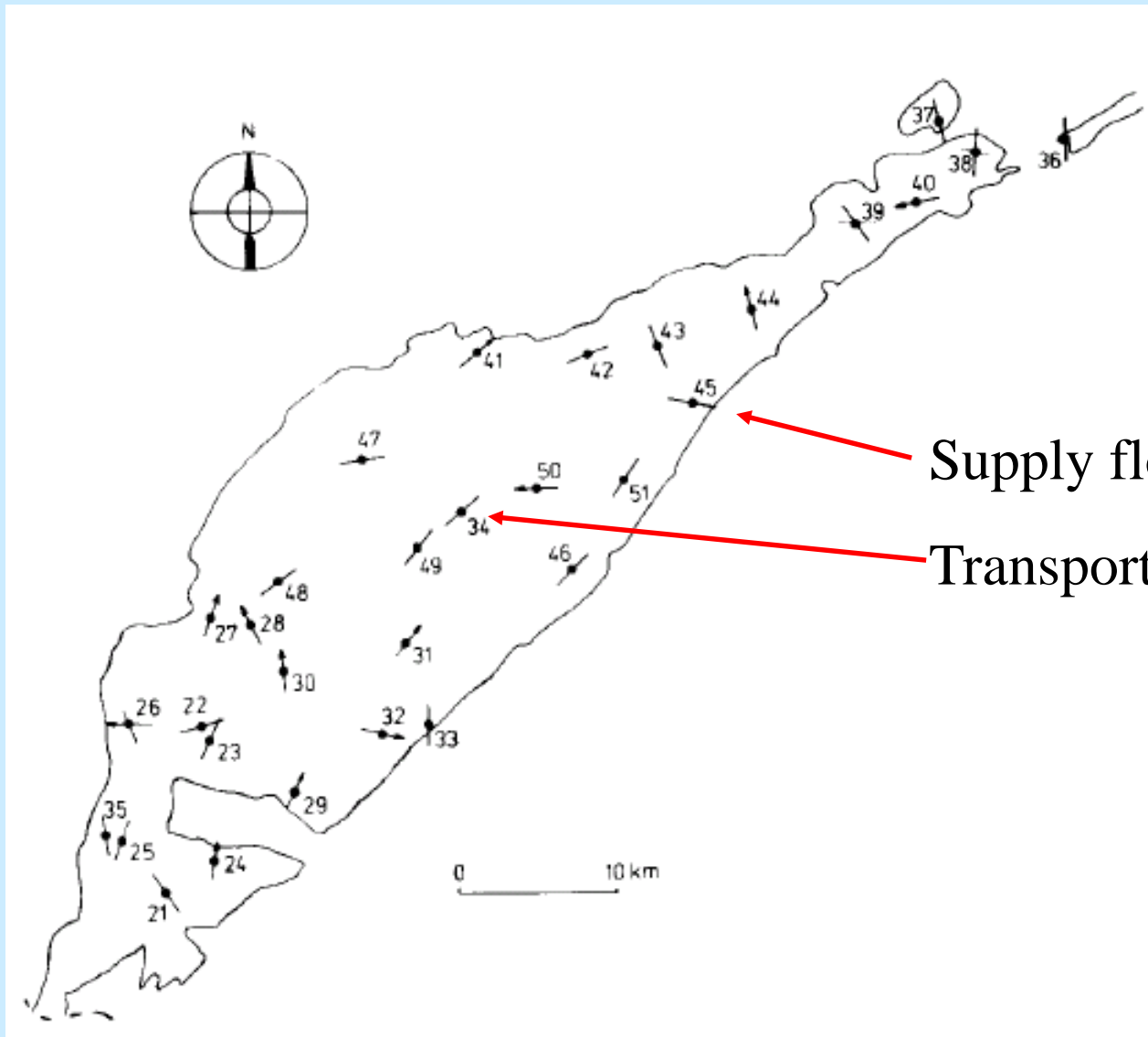
Ždánice Formation

Magura Flysch



relatively good correlation in both cases

Palaeogeography of Ždánice – Hustopeče Formation

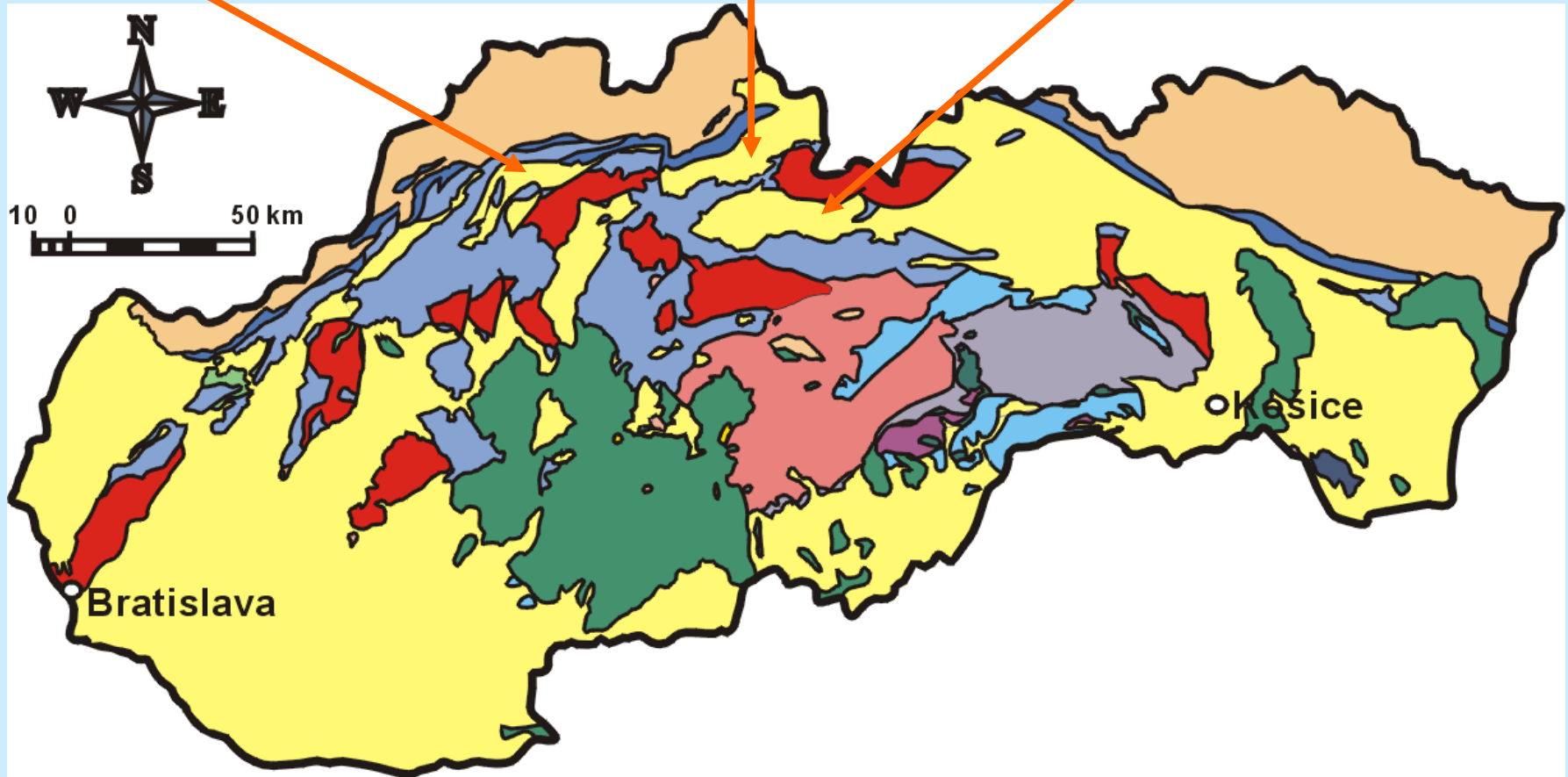


Supply flow

Transport along basin

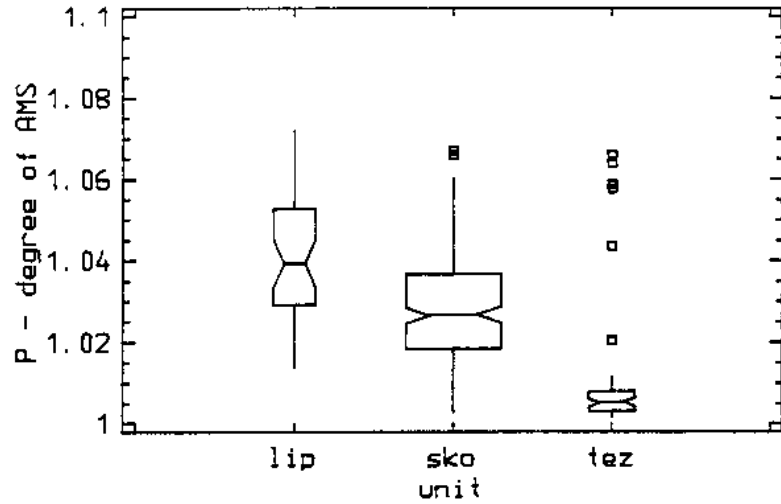
Geol map of Slovakia

Zázrivá Depression Skorušinské vrchy Hill Liptov Depression

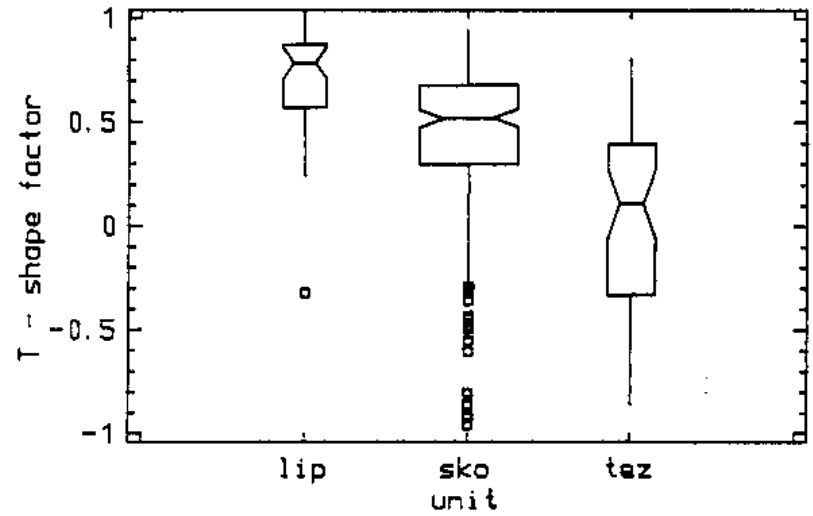


P, *T* and *f* Parameters

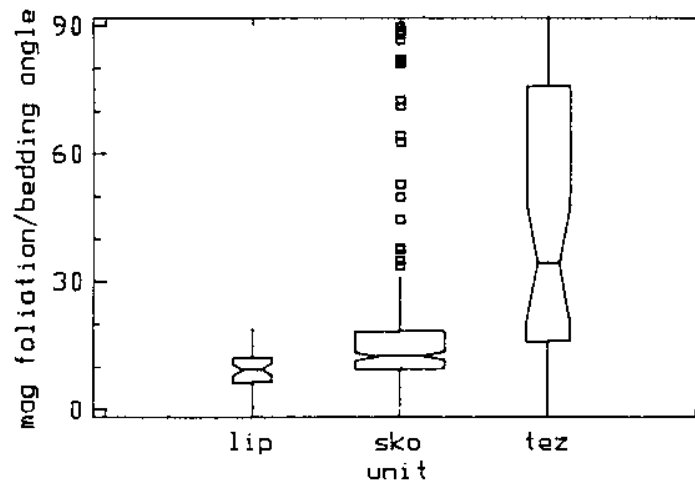
Intracarpathian Palaeogene



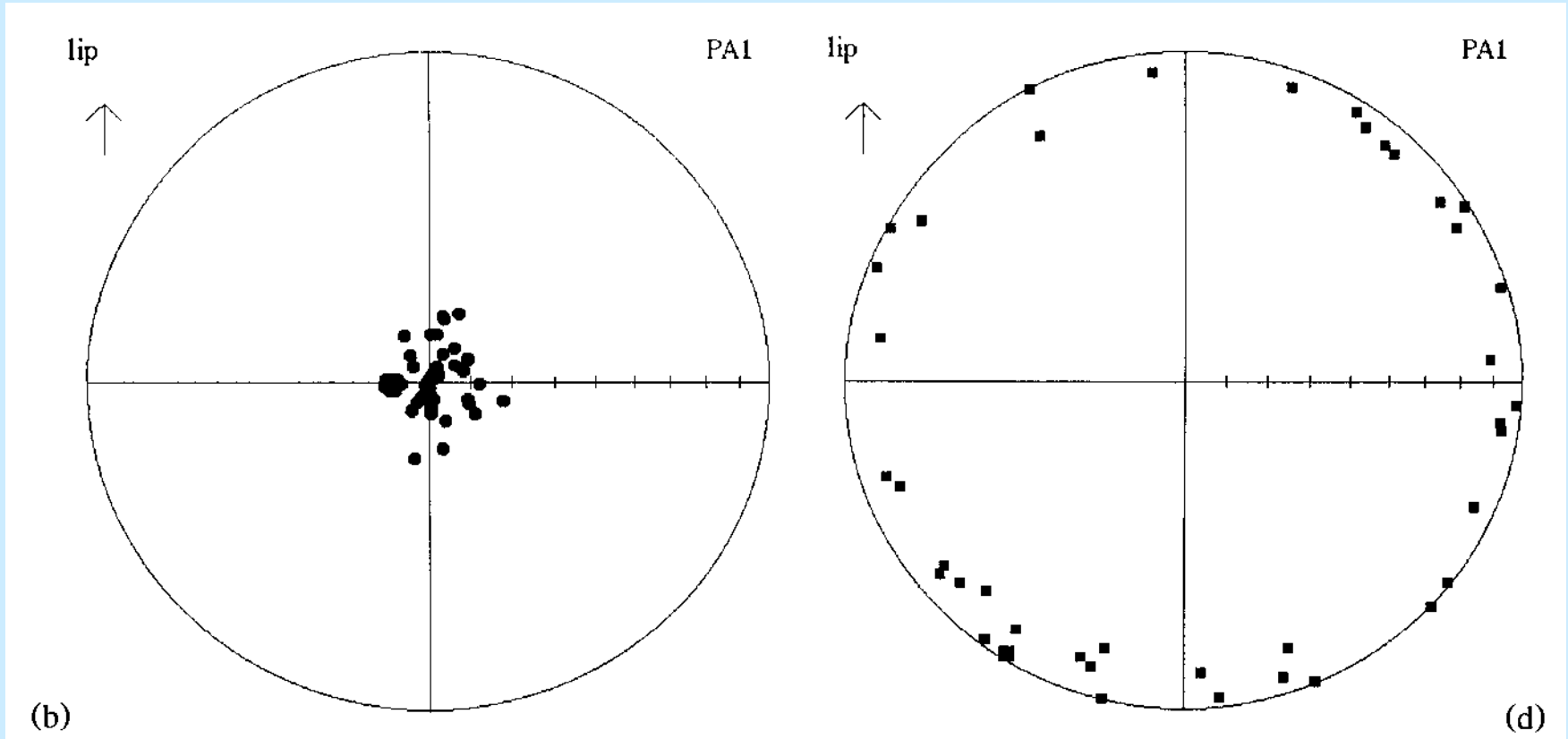
Intracarpathian Palaeogene



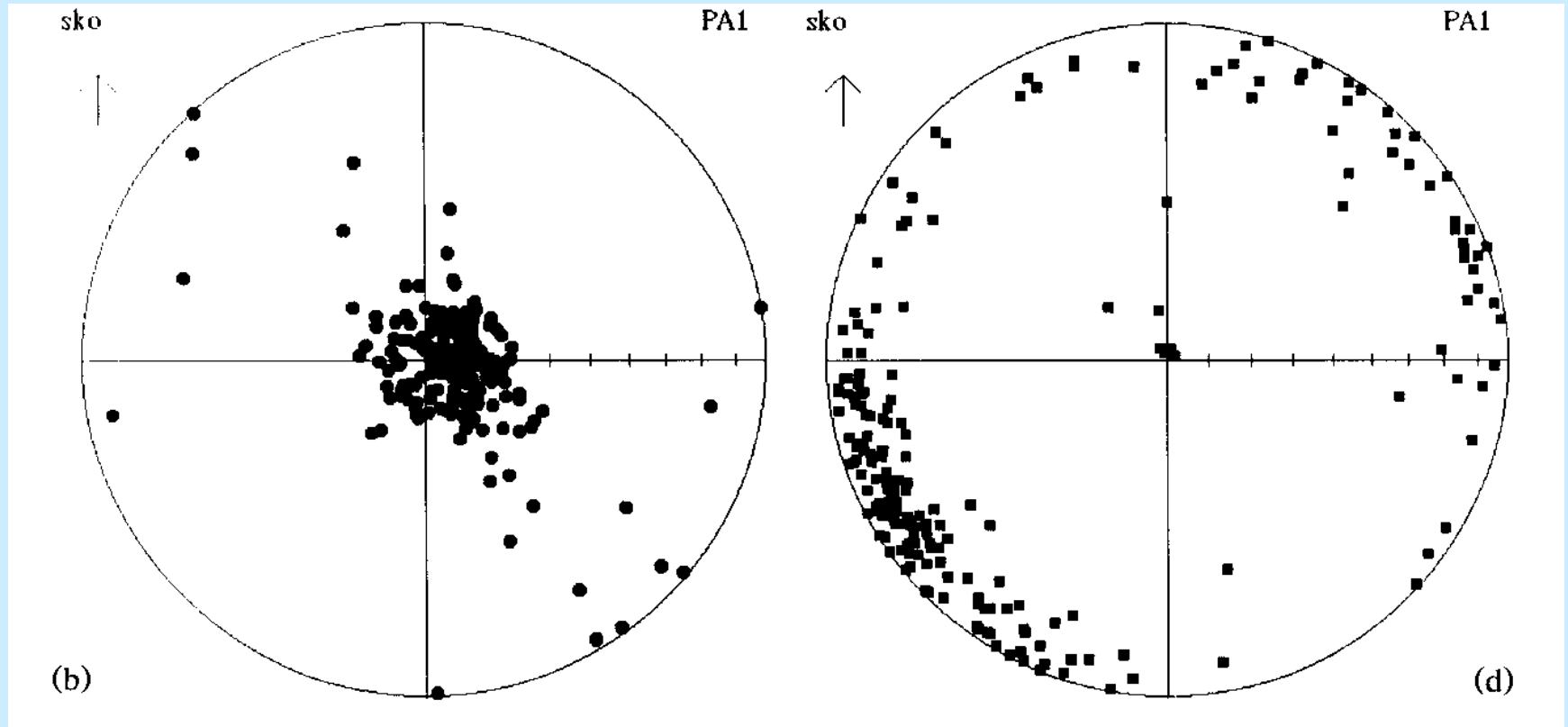
Intracarpathian Palaeogene



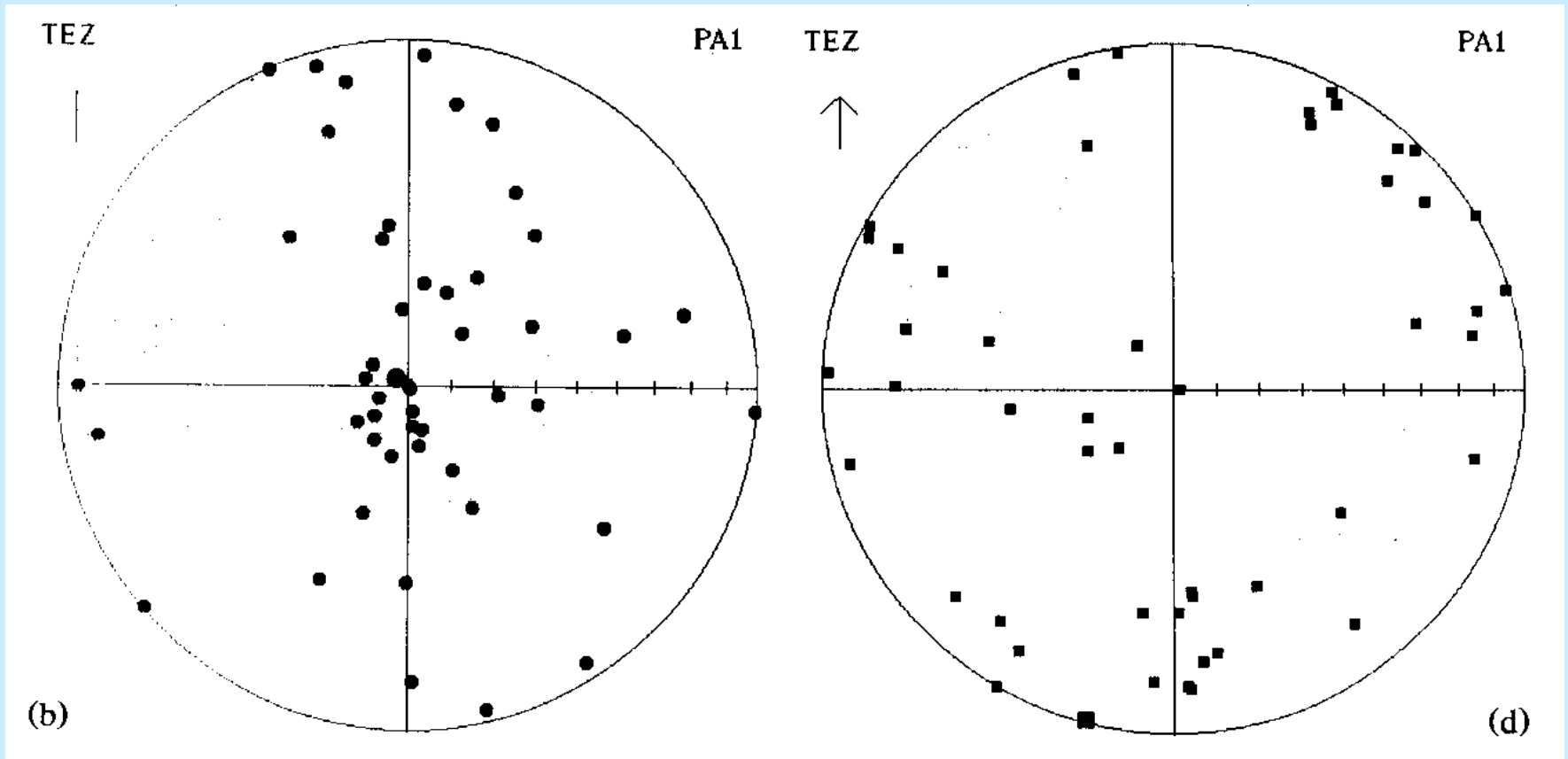
Liptovská kotlina - Pa



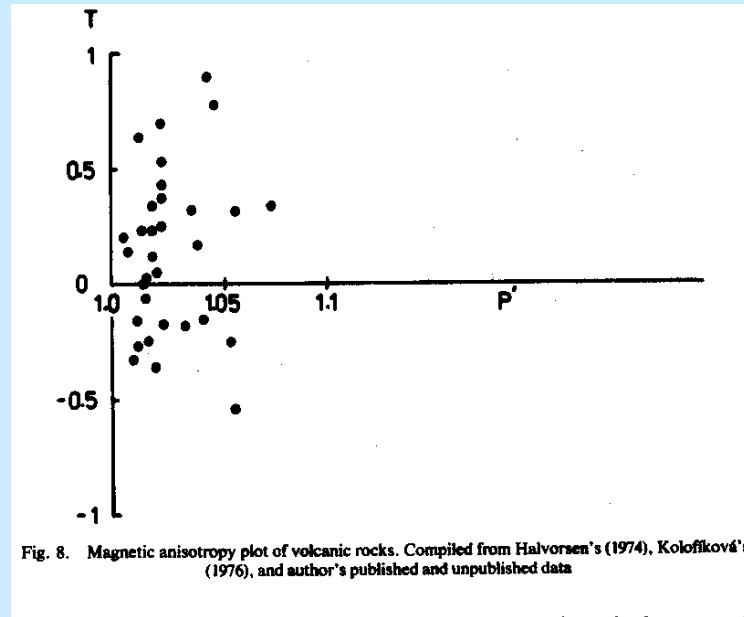
Skorušinské vrchy - Pa



Zázrivská deprese - Pa



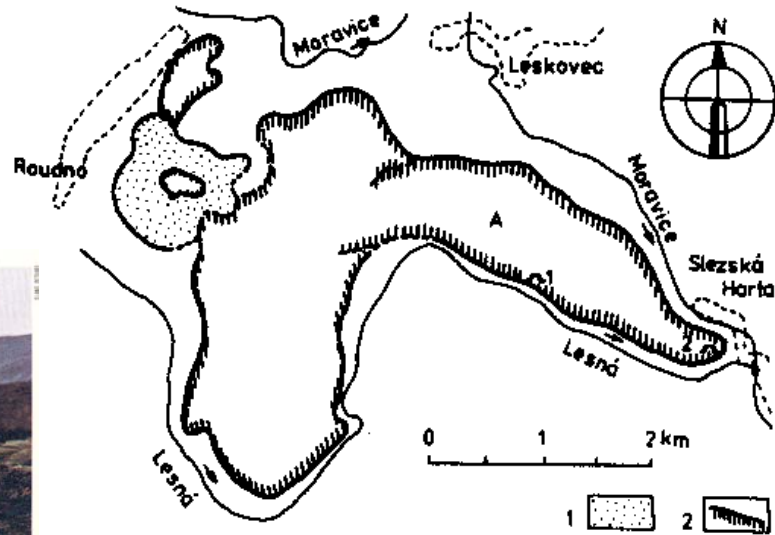
VOLCANICS AND DIKES



Degree of AMS is extremely low, typically $P < 1.05$, indicating very weak preferred orientation not detectable classically

Magnetic foliations and lineations are related to lava flow directions

LAVA FLOWS (Chřibský les L.F.)



Geological map of the Chřibský les lava flow (A) and its environs. (1) basalt tuff, (2) series of lava bodies. After Kolofíková (1976). Courtesy of the author.



68 A new flow of smooth-surfaced lava (pahoehoe) covering old, rough-surfaced lava (aa), Hawaii

35

Quaternary in age, flew in ancient valley of the Moravice river, flow direction is therefore very well known

Orientations

K1 || flow direction

random orientation

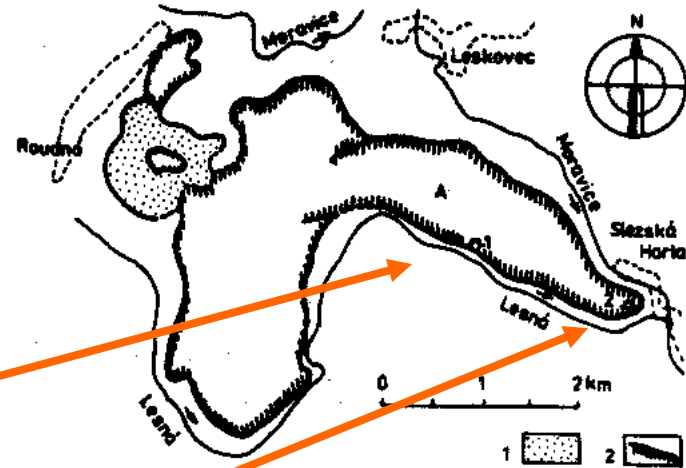


Fig. 9. Synoptic geological map of the Chřibský les lava flow (A) and its environs. (1) basalt tuff, (2) boundaries of lava bodies. After Kolářková (1976). Courtesy of the author.

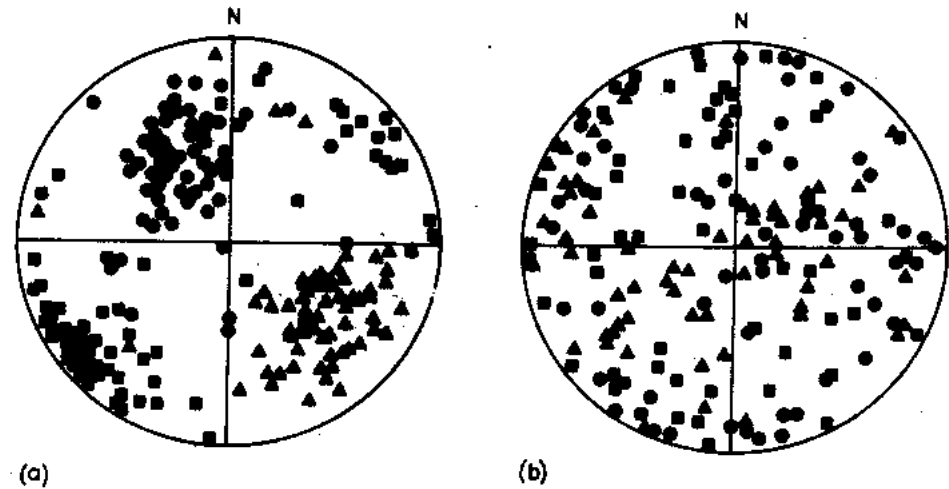


Fig. 10. Directions of principal susceptibilities in two sampled sites of the Chřibský les lava flow. (a) quarry 1, (b) quarry 2. ▲: maximum susceptibility direction, ■: intermediate susceptibility direction, ●: minimum susceptibility direction. After Kolářková (1976). Courtesy of the author.

DIKES

(after Raposo & Ernesto, PEPI 1995)

Focus is on the relationship of the MF and ML to dike shape

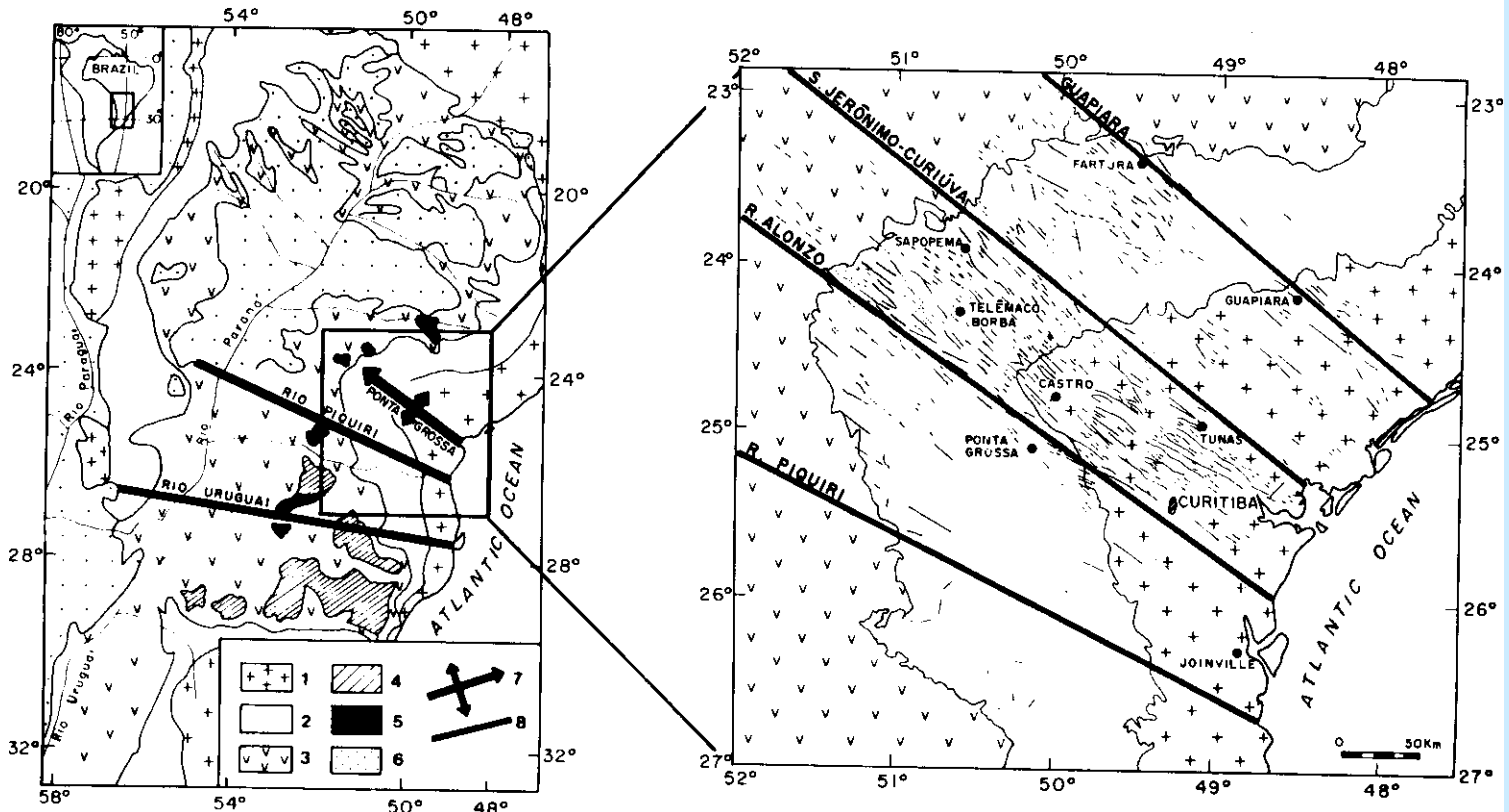


Fig. 1. Generalized geological map of the Paraná Basin showing the Ponta Grossa Arch: (1) crystalline basement; (2) pre-volcanic sediments (mainly Palaeozoic); (3) basic to intermediate flood volcanics from the Serra Geral Formation; (4) acid lava flows (Palmas type); (5) acid lava flows (Chapecó type); (6) post-volcanic sediments (mainly upper Cretaceous); (7) arch-type structure; (8) tectonic and/or magnetic lineaments.

AMS Types

Type I: K3 | dike plane

a) K1 horizontal

b) K1 vertical

free flow

Type II: K3, K1 || dike plane

a) K1 horizontal

b) K1 vertical

Type III:

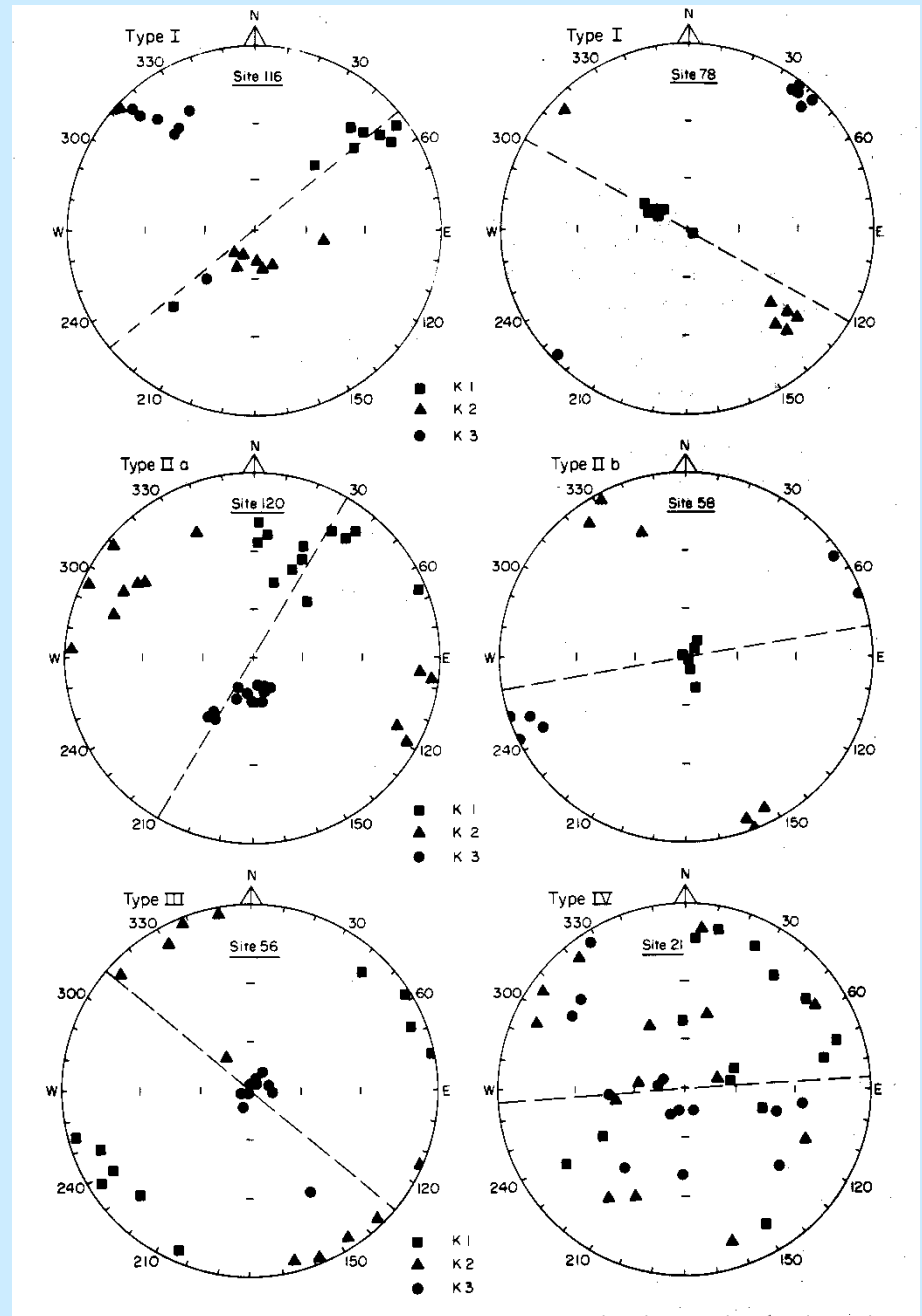
K3||, K1 | dike plane

static compaction

Type IV:

random orientation in K1, K3

partially solidified lava



SILL vs. RING DIKE

(after Halvorsen, EPSL, 1974)

Bastian a Ronnbeck Islands create an elliptic formation

Two hypotheses for its origin:

1. islands are remanants of an irregularly sunken sill
2. islands are remnants of a Ring Dike

Expectations:

- horizontal MF in case 1
- steep MF in case 2

Method:

AMS of the islands plus
AMS of a doubtless sill

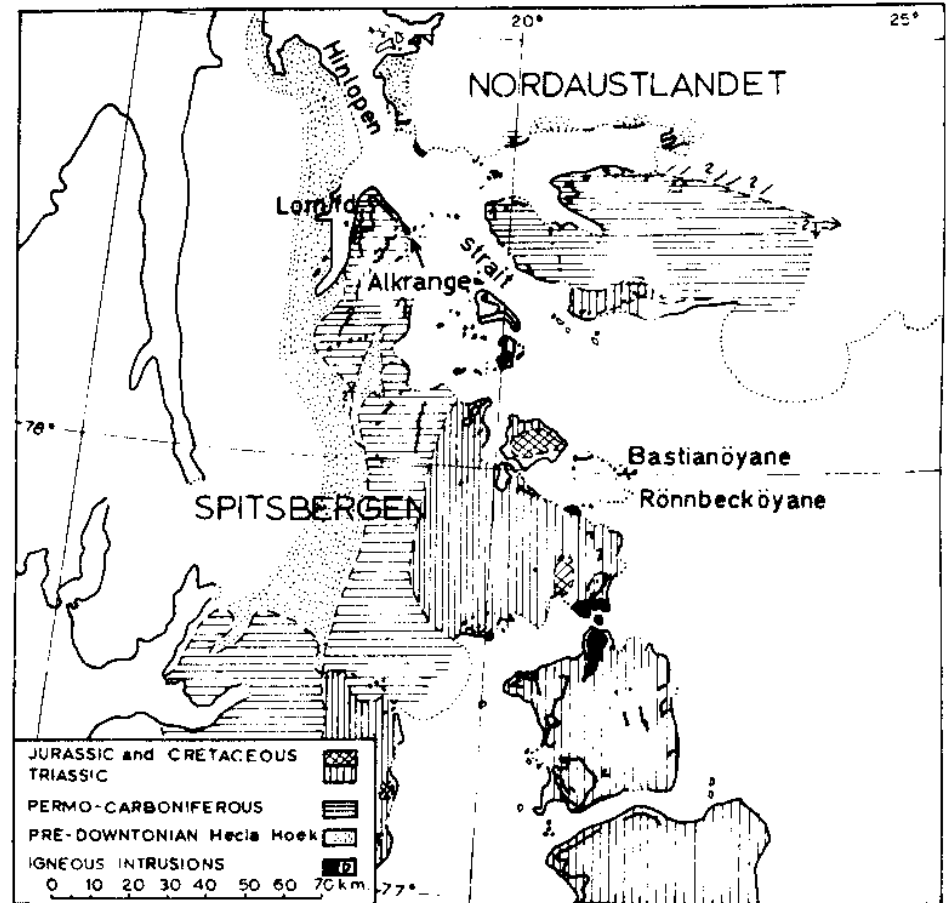


Fig. 11. Geological sketch map of the Hinlopen strait, Spitsbergen. After Halvorsen (1974). Courtesy of Elsevier Publishing Company.

Geol. Scheme

Sill

Islands

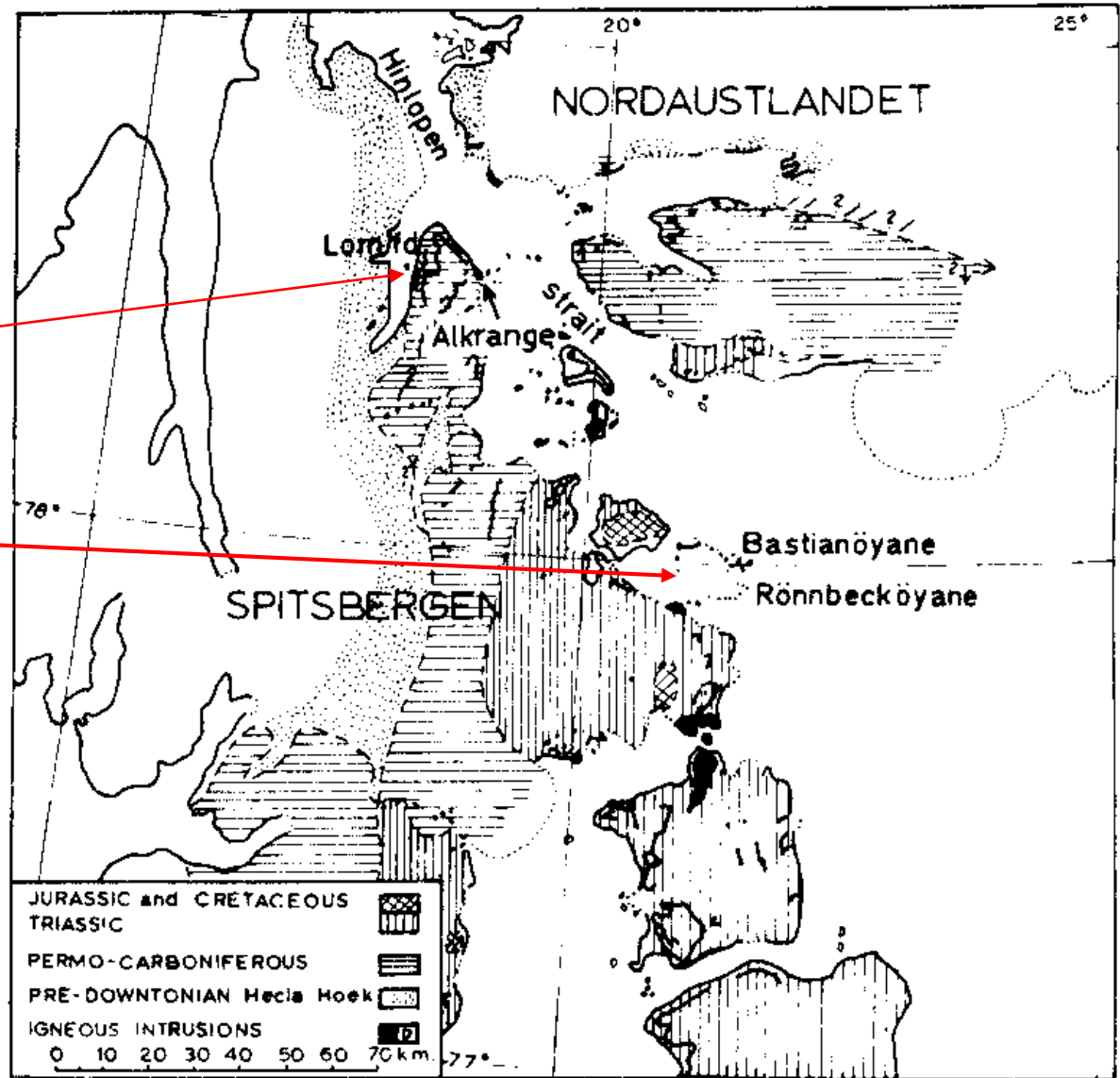
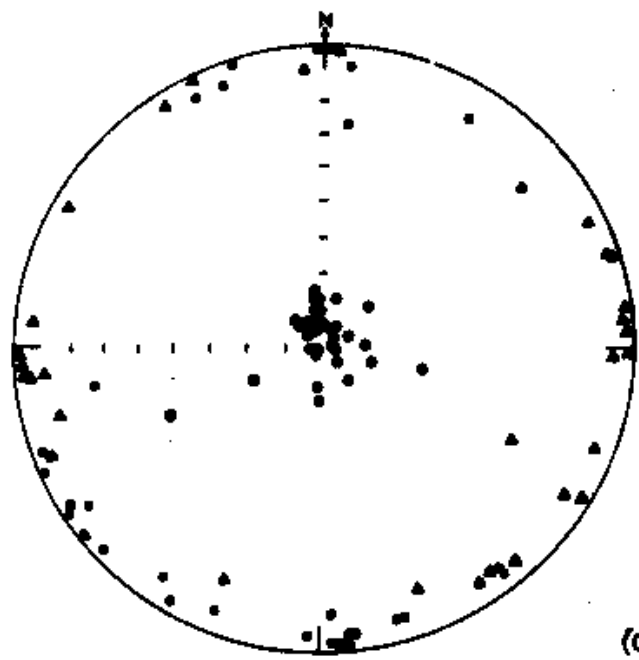


Fig. 11. Geological sketch map of the Hinlopen strait, Spitsbergen. After Halvorsen (1974). Courtesy of Elsevier Publishing Company.

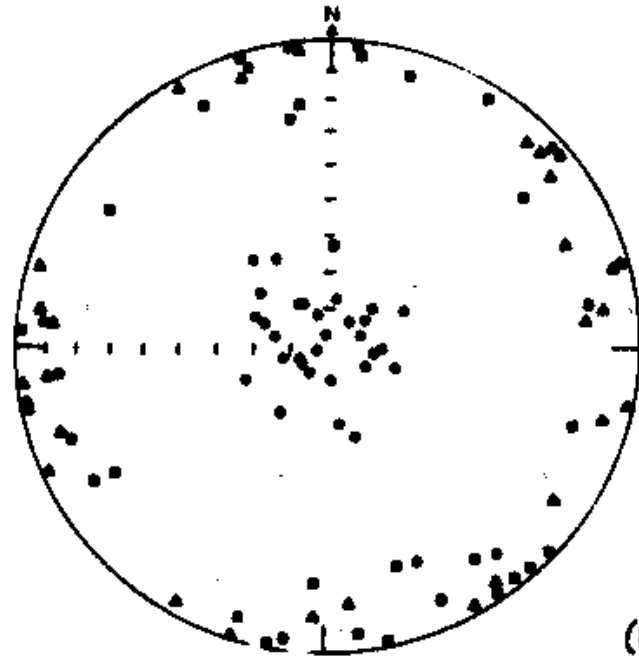
Principal Directions

Lomfjorden Sill

Bastian and Ronnbeck islands



(a)

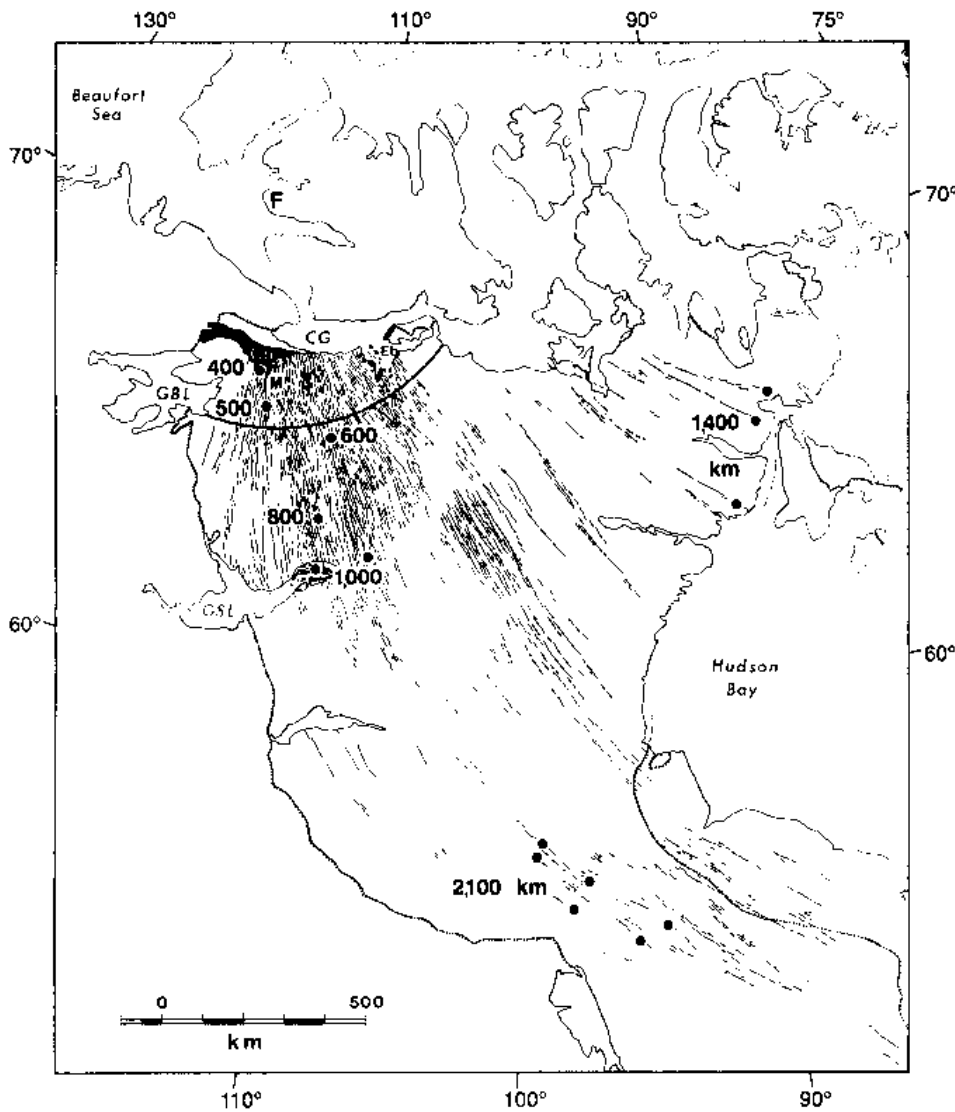


(b)

Fig. 12. Directions of principal susceptibilities in the Lomfjorden sill (a) and in the Bastian and Rönbeck islands (b). After Halvorsen (1974). Courtesy of Elsevier Publishing Company.

Bastian and Ronnbeck Islands are remnants of an irregularly sunken sill rather than remnants of a ring dike.

DIKES ABOVE MANTLE PLUMES



McKenzie Radiating Dike Swarm

sampling at several
distances from swarm
center, at 400, 500, 600,
800, 1000, 2000 km.

Magnetic Foliations and Lineations

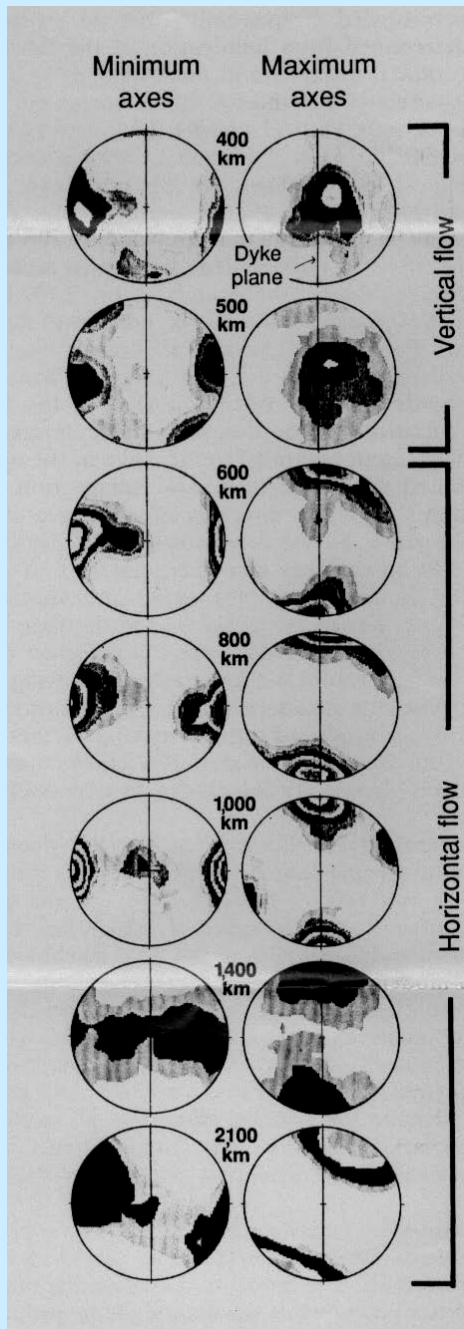
Vertical flow at distances ≤ 600 km.

Horizontal flow at distances > 600 km

Complex AMS patterns at very large distances.

Conclusions:

Assuming that lava flows vertically above the mantle plume, then mantle plume under the MacKenzie dike swarm is much smaller in diameter than is the plume diameter. The lava flows vertically above the plume, but in upper levels its flow changes into horizontal.



ČISTÁ-JESENICE PLUTON

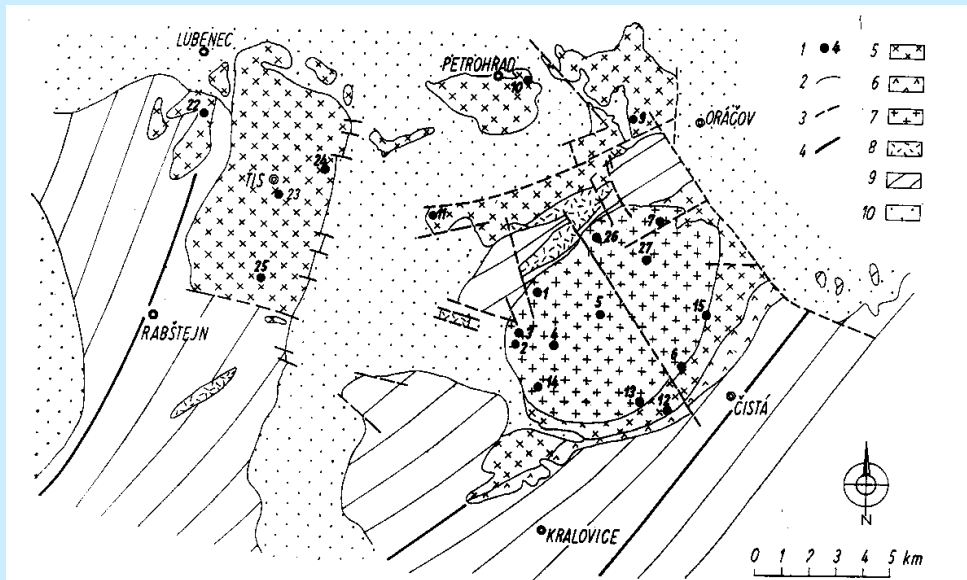
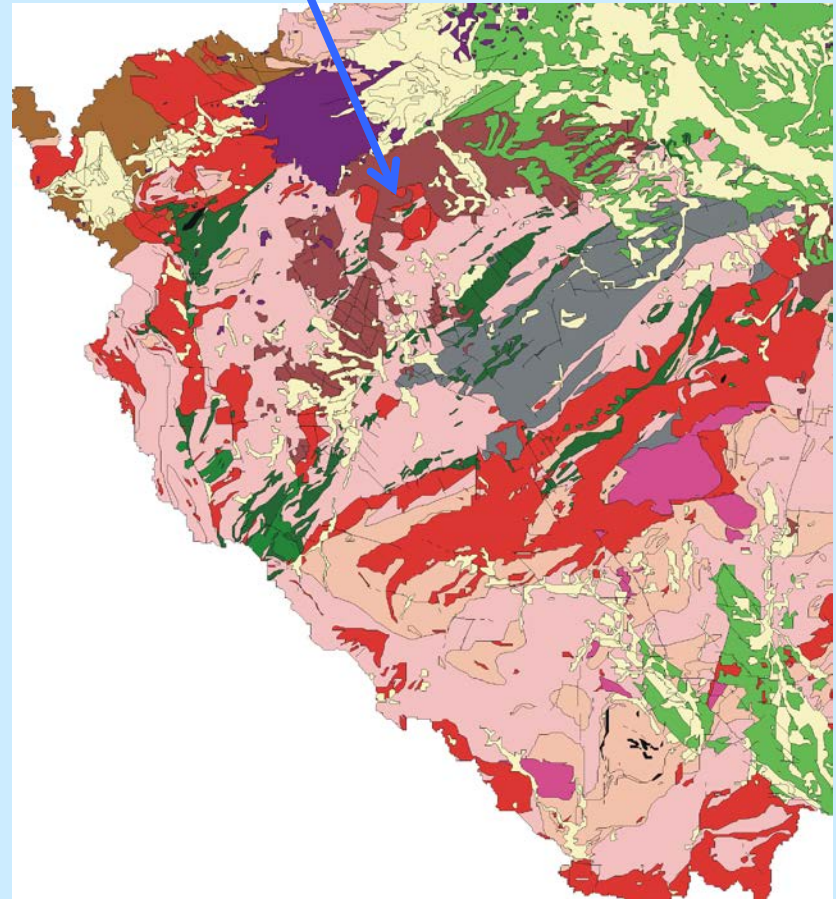
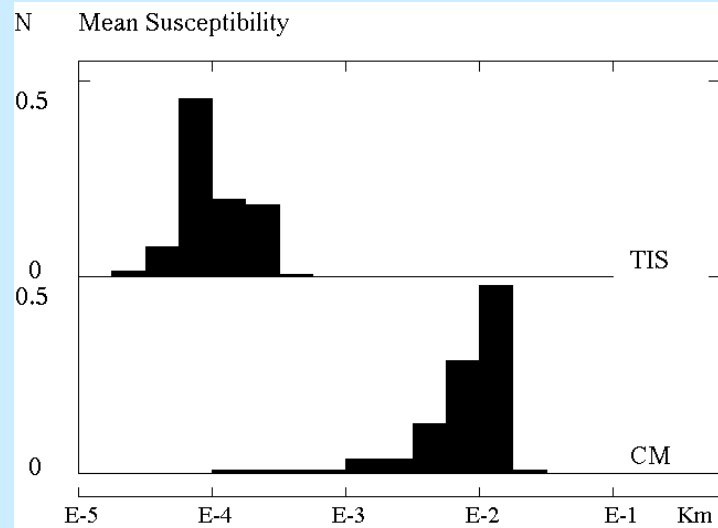
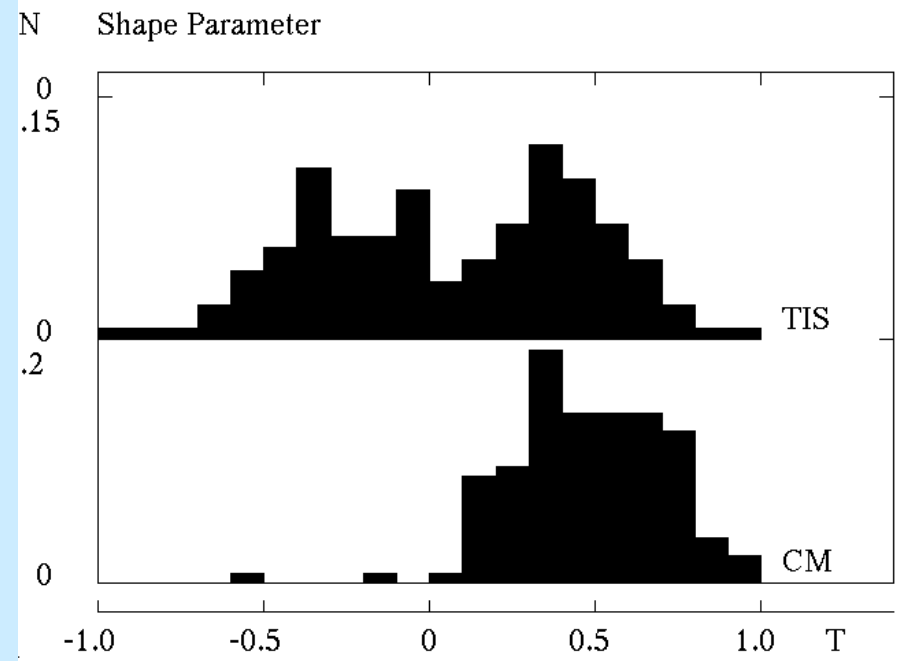
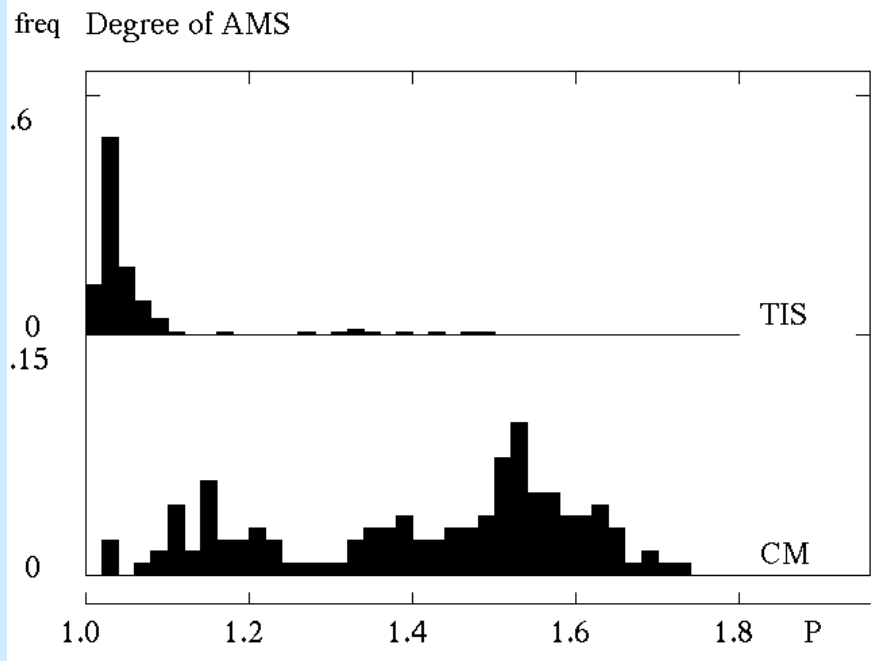


Fig. 1. Synoptic map of the Čistá—Jesenice massif and surrounding formations with collection sites plotted, compiled from BRETŠNAJDR [2], HOLUBEC [6], KLOMÍNSKÝ [13], ZOUBEK [17]; 1 — collection sites, 2 — boundaries between rocks, 3 — faults, 4 — course of the main Proterozoic structures (mentioned in the text), 5 — Tis granite, 6 — auto-metamorphosed facies of the Tis granite, 7 — Čistá granodiorite, 8 — young volcanics, 9 — Proterozoic, 10 — Permo-Carboniferous



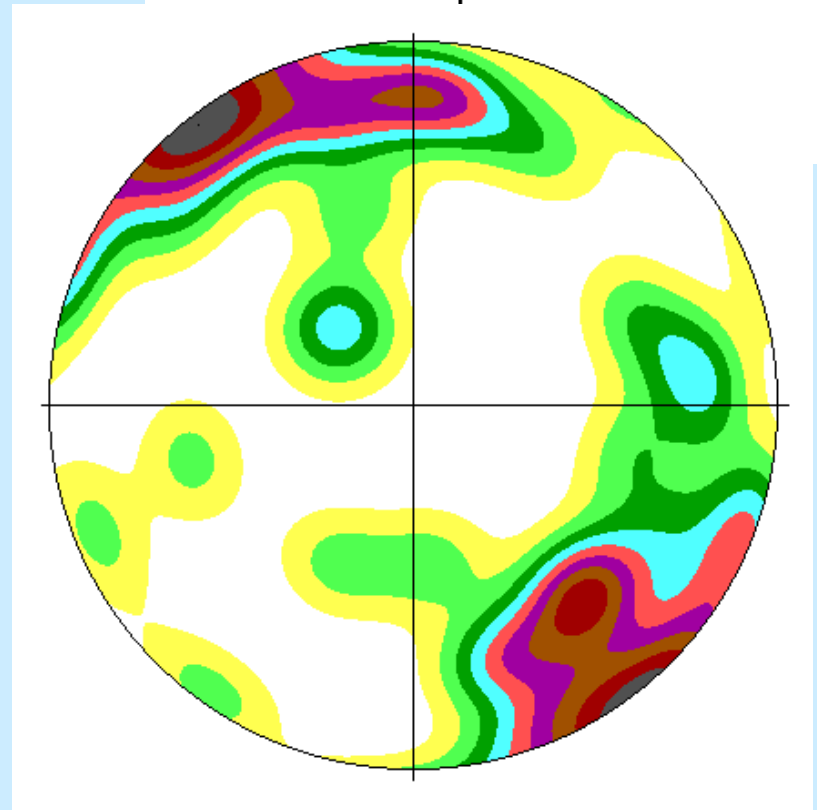
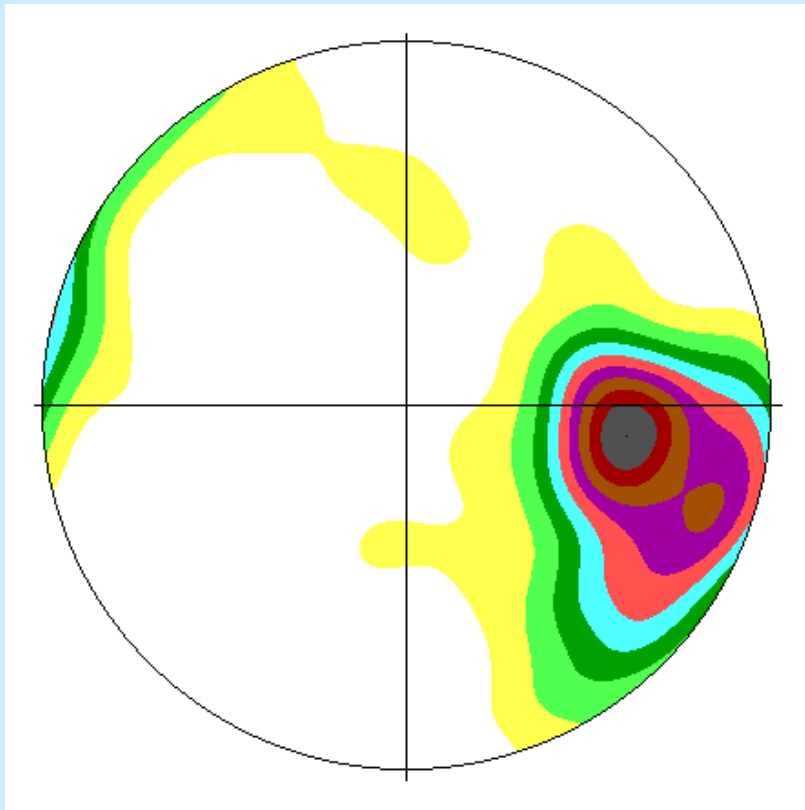
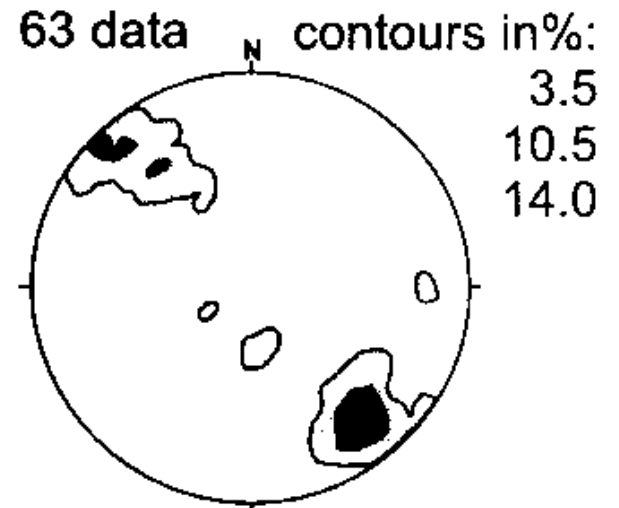
AMS Parameters



Tis Granite: MF

W body

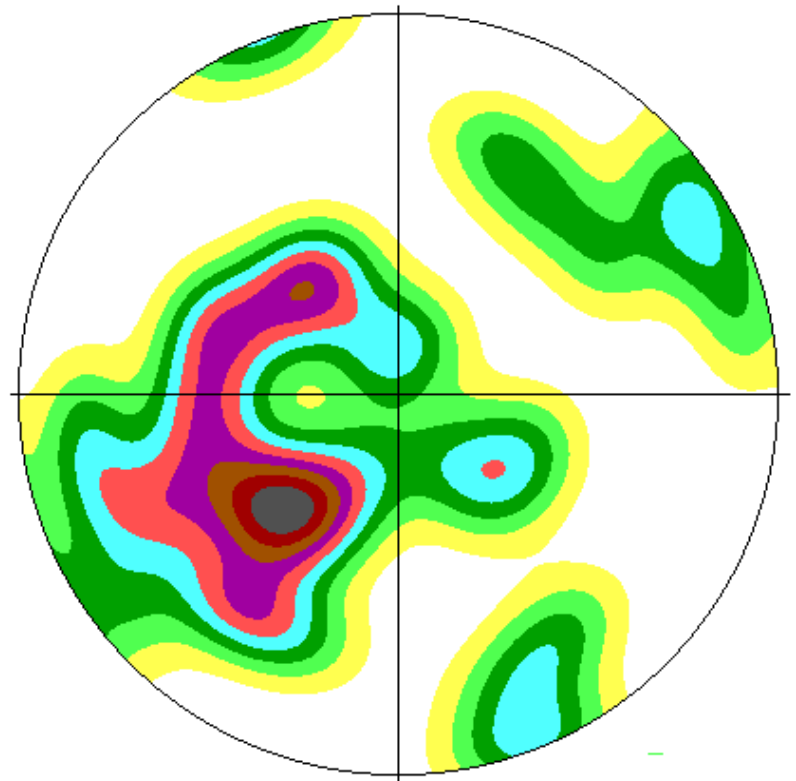
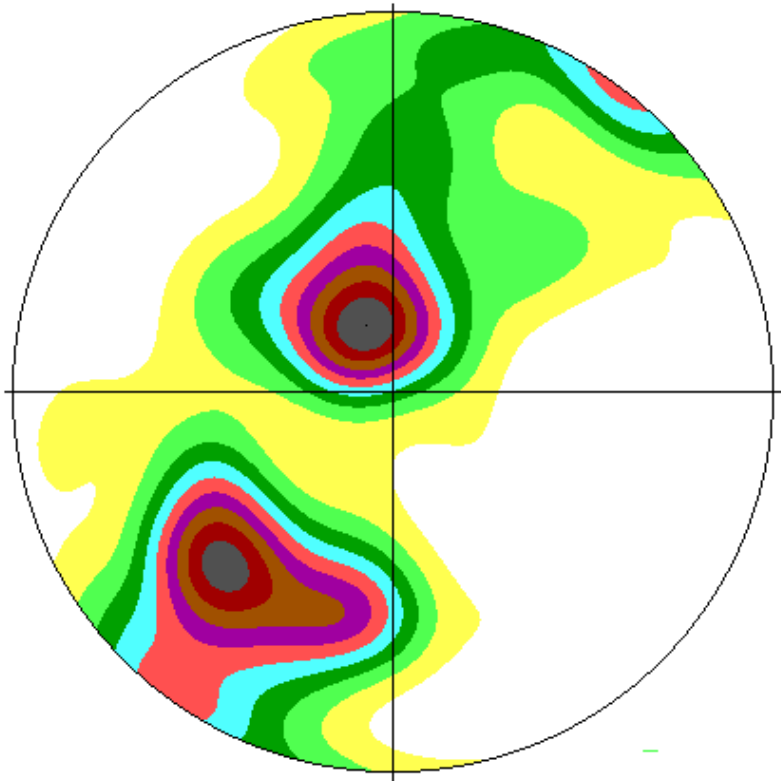
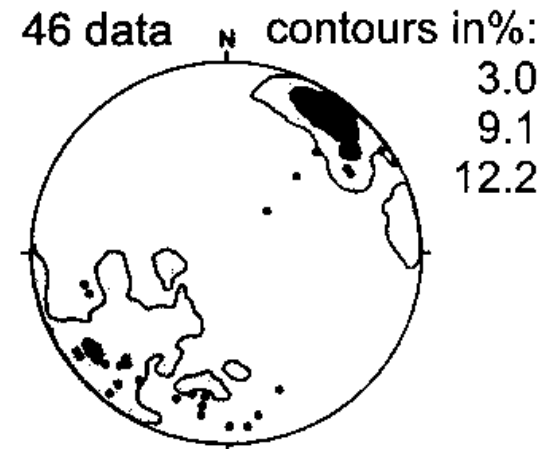
E body



Tis Granite: ML

W body

E body



Čistá stock: AMS Orientation

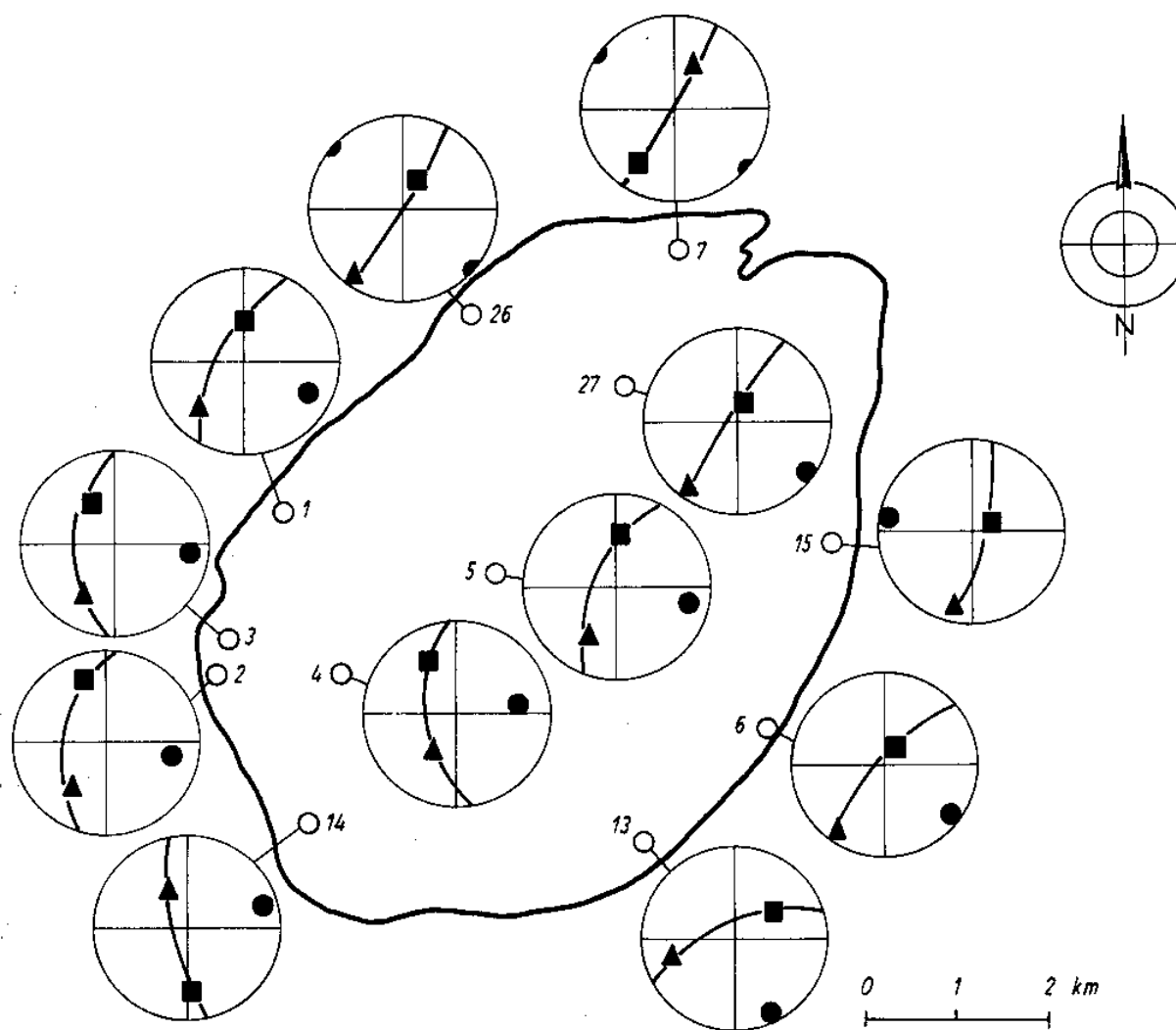


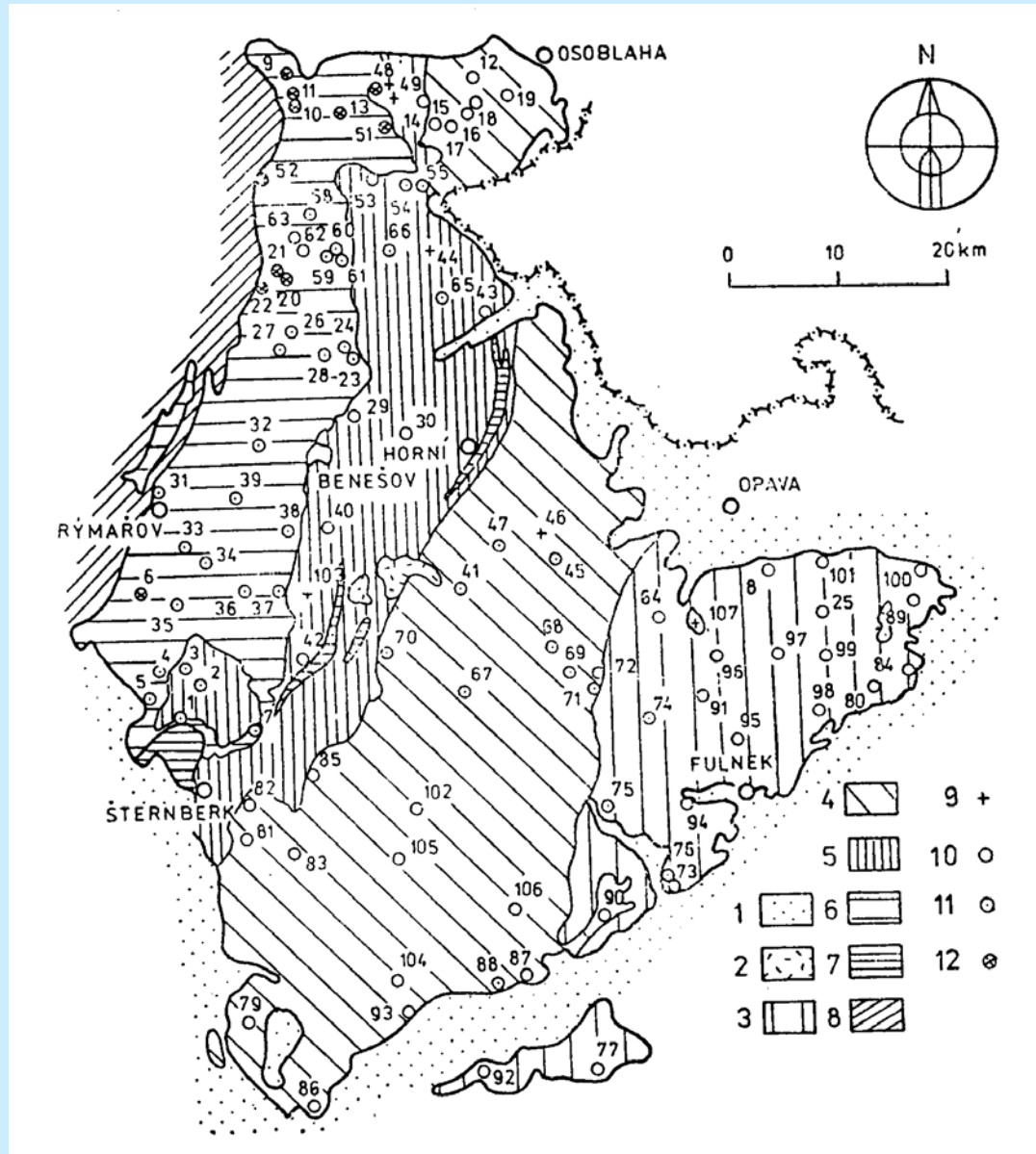
Fig. 4. Mean directions of principal susceptibilities in individual localities of the Čistá granodiorite stock; great circles: magnetic foliation

AMS AND CLEAVAGE

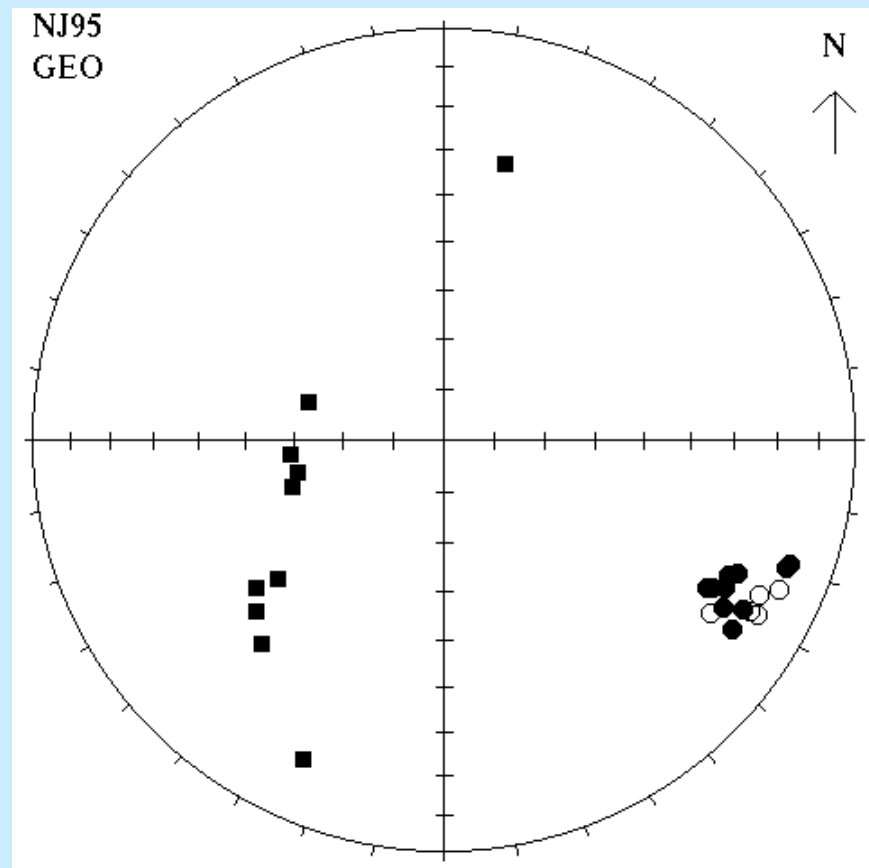
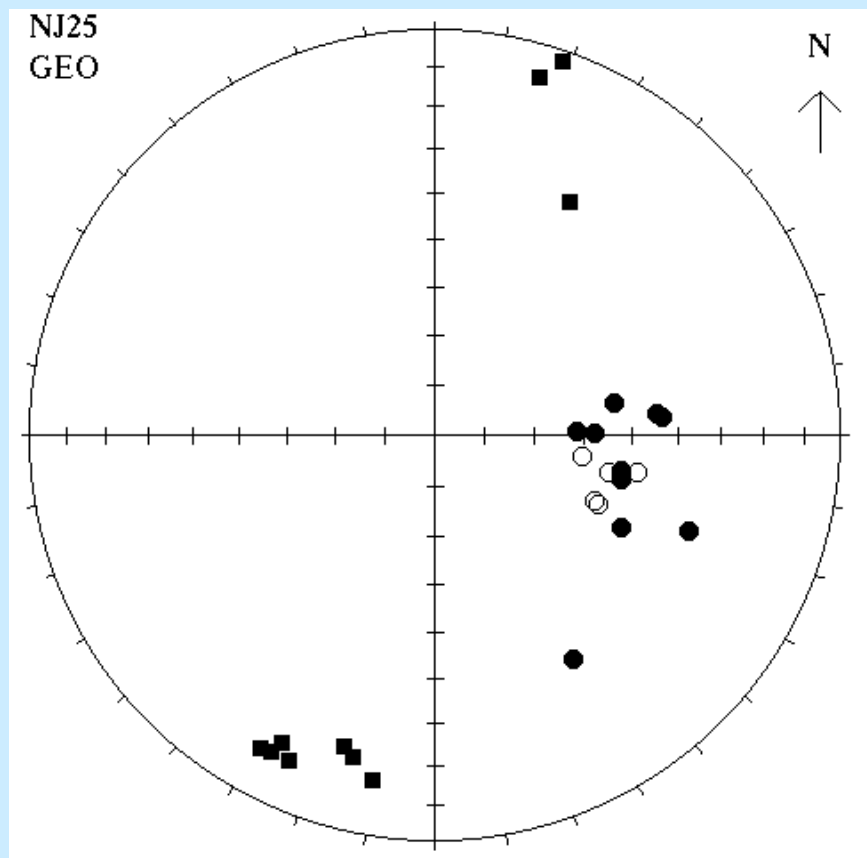


*Axial plane cleavage, Mesozoic marls. Helvetic Alps, Valais, Switzerland.
(Photograph by J. McManus.)*

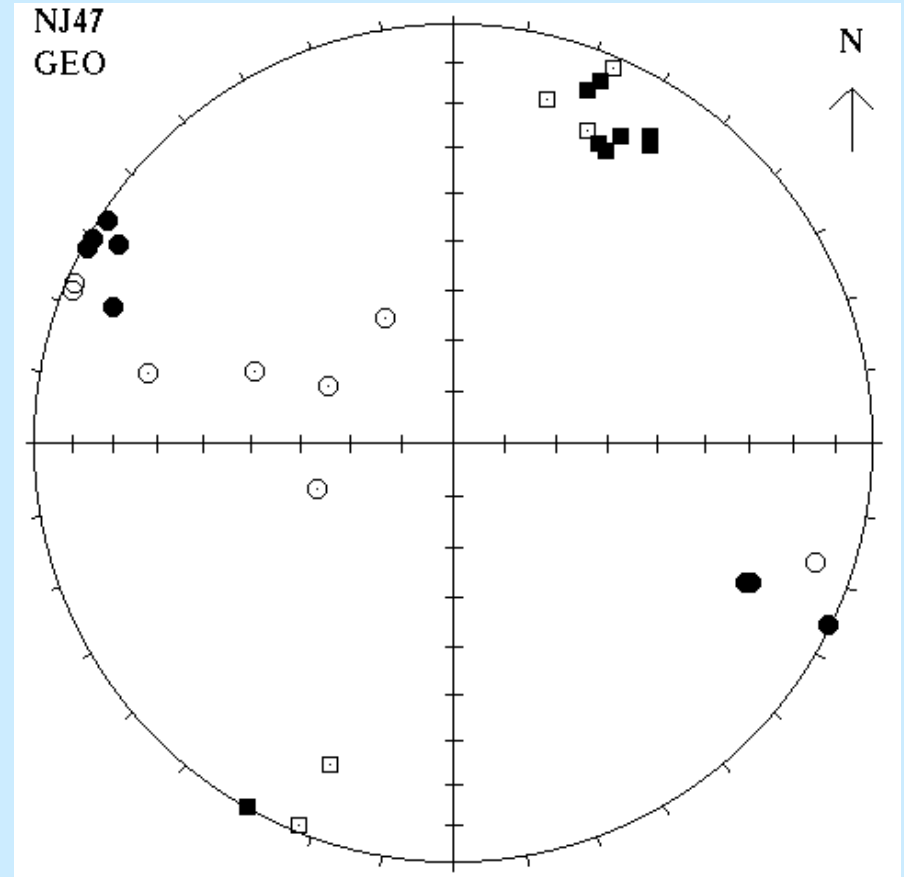
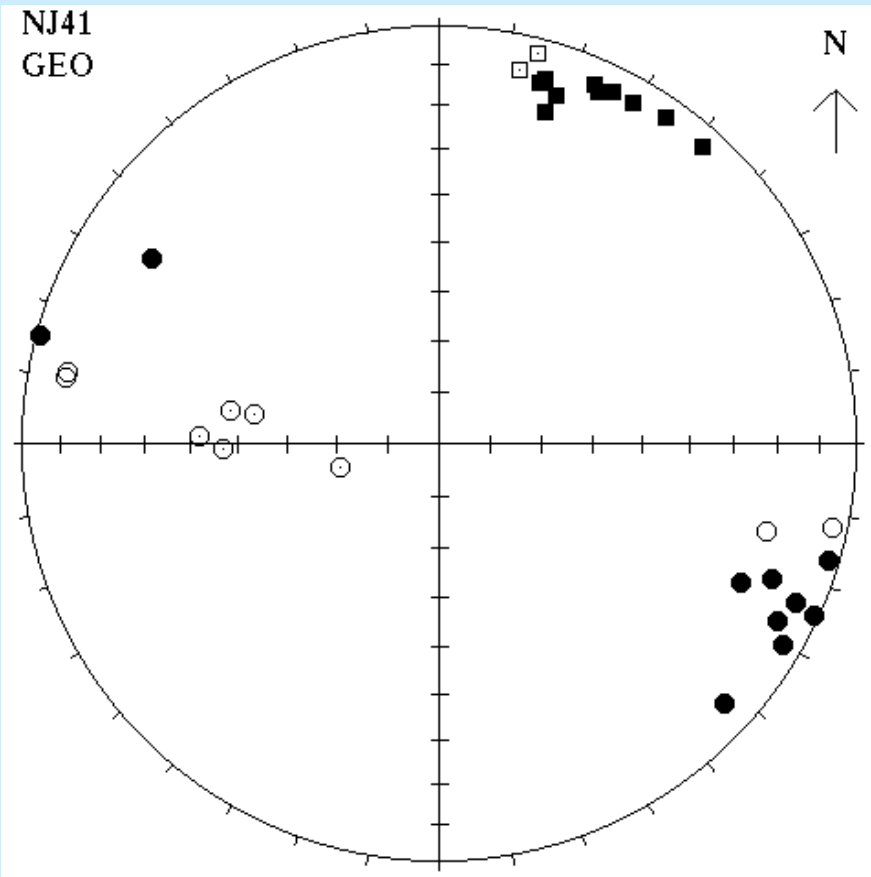
Nížký Jeseník - geol. scheme



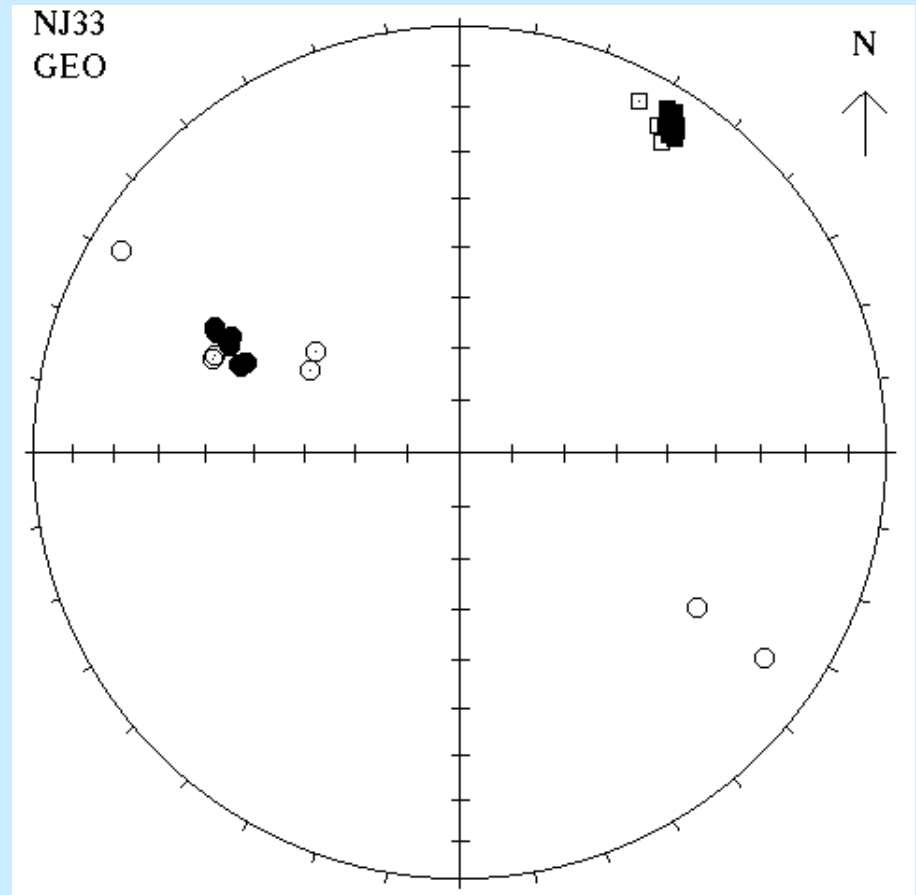
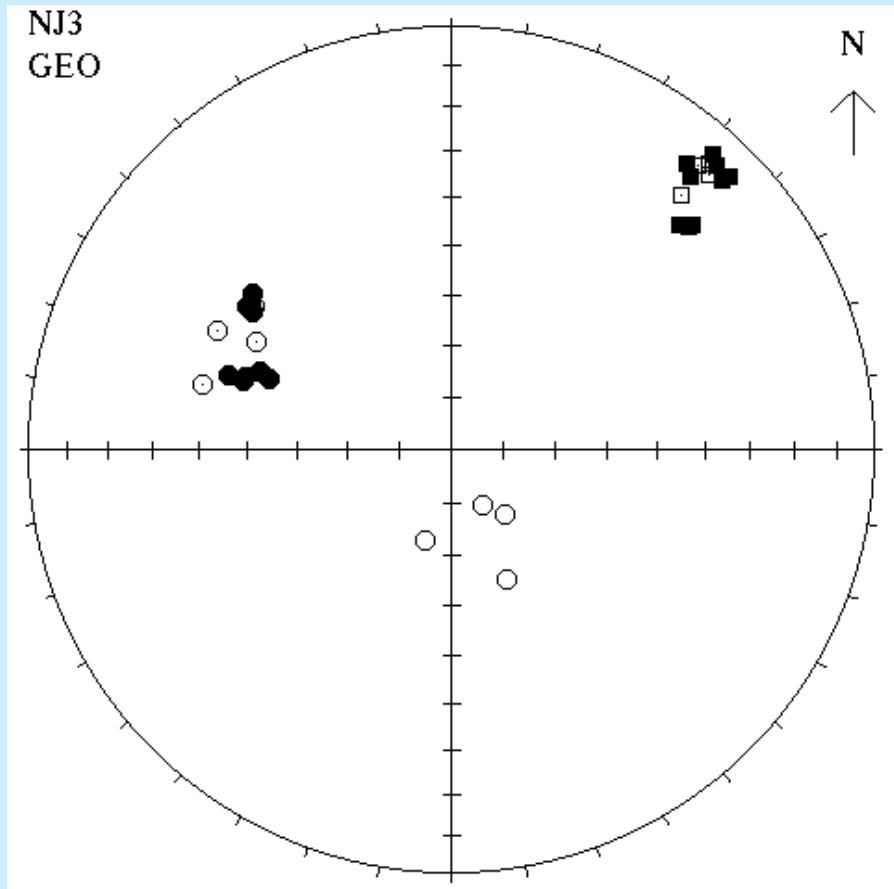
Bedding only



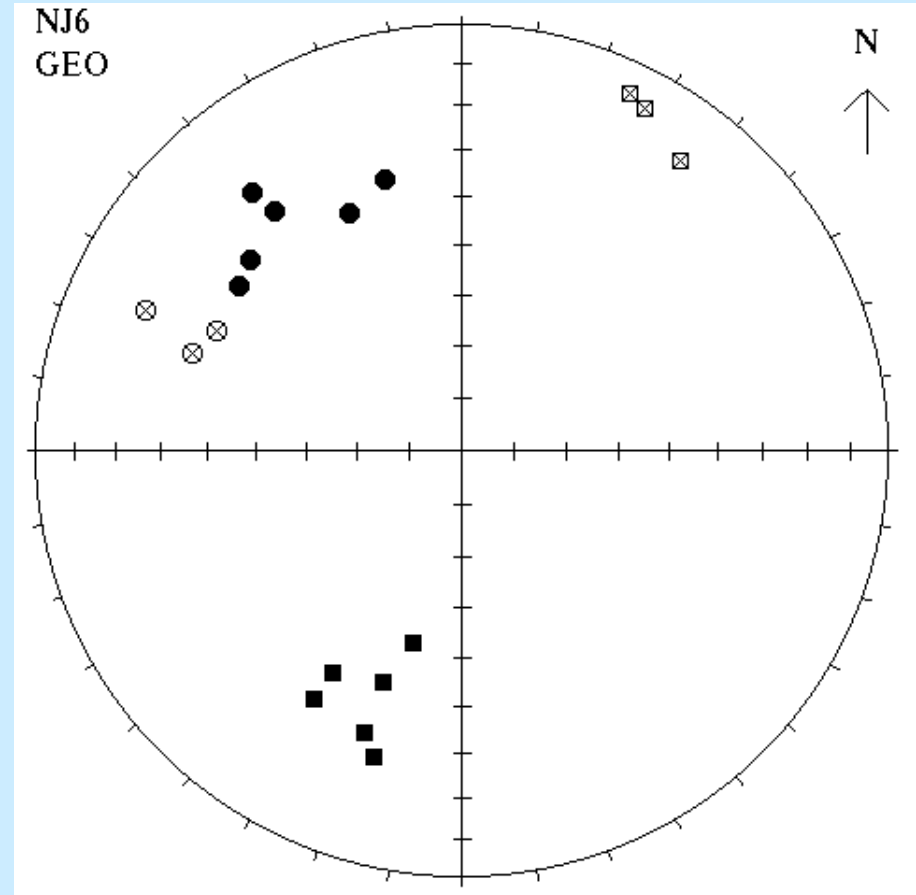
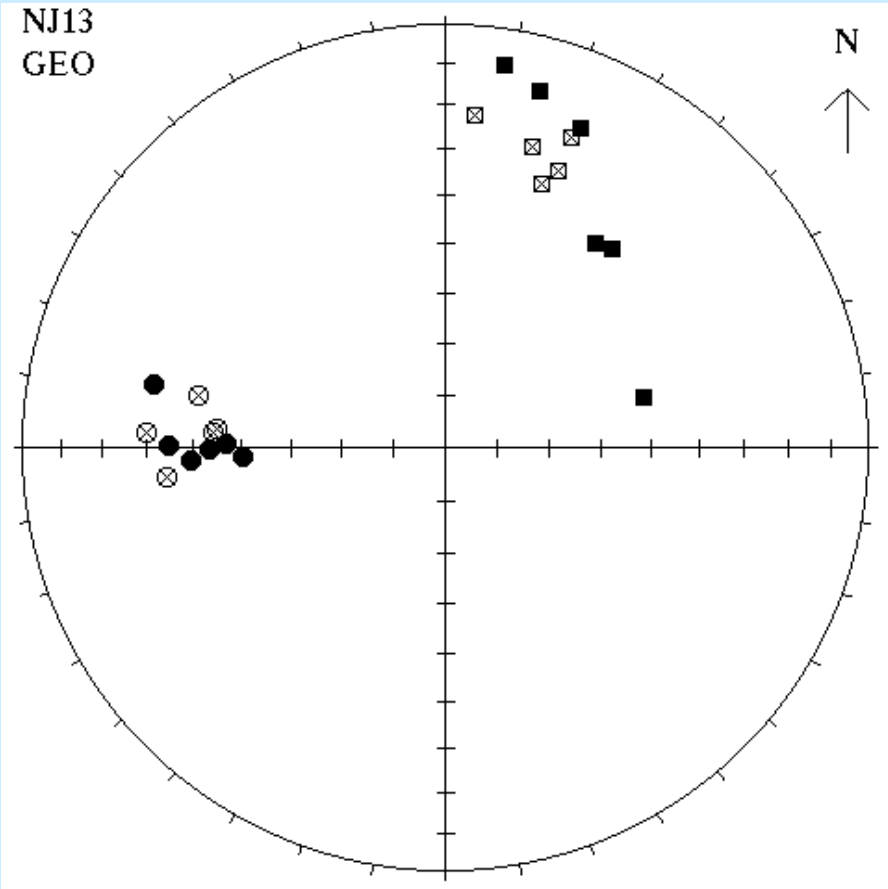
Spaced Cleavage



Slaty Cleavage

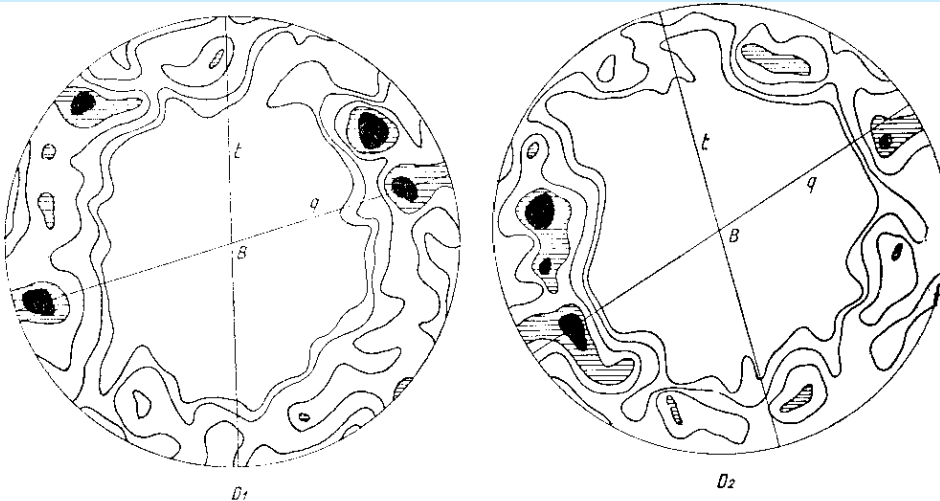
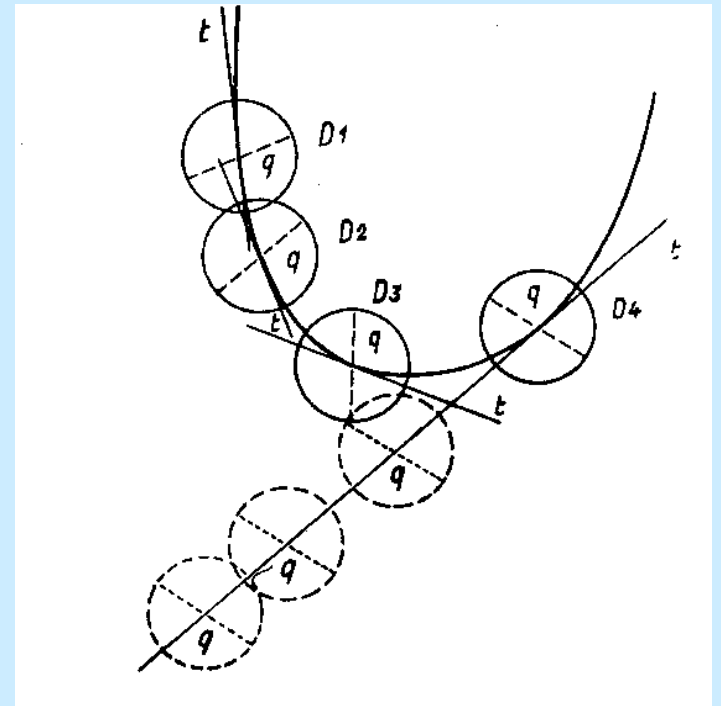


Metamorphic Schistosity



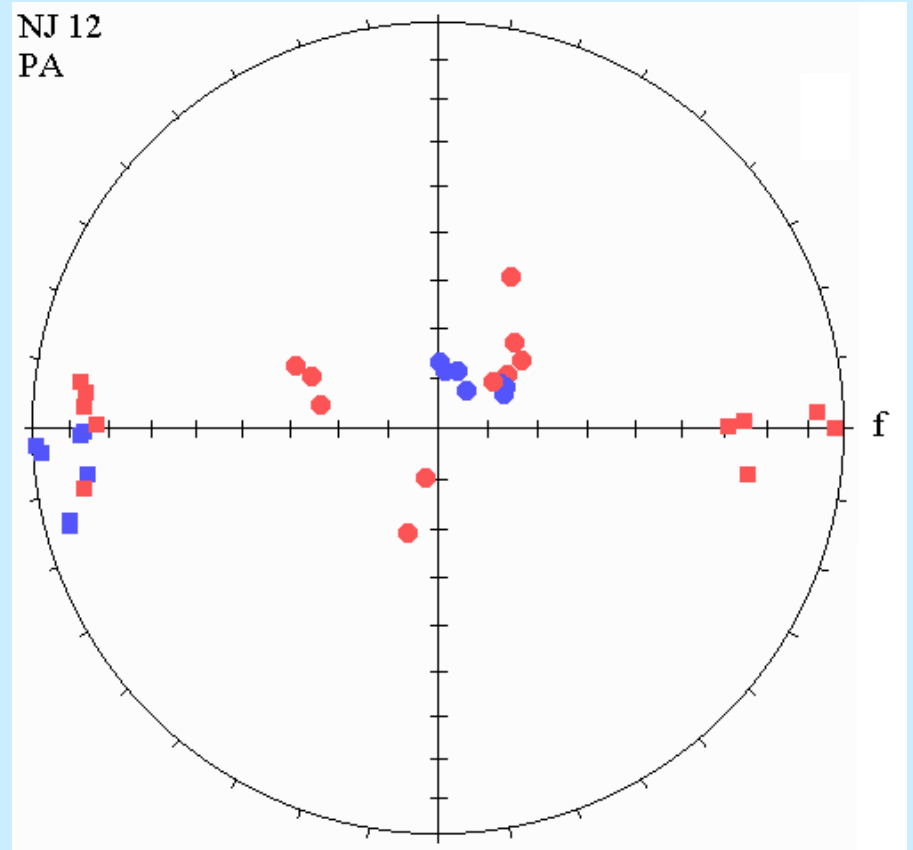
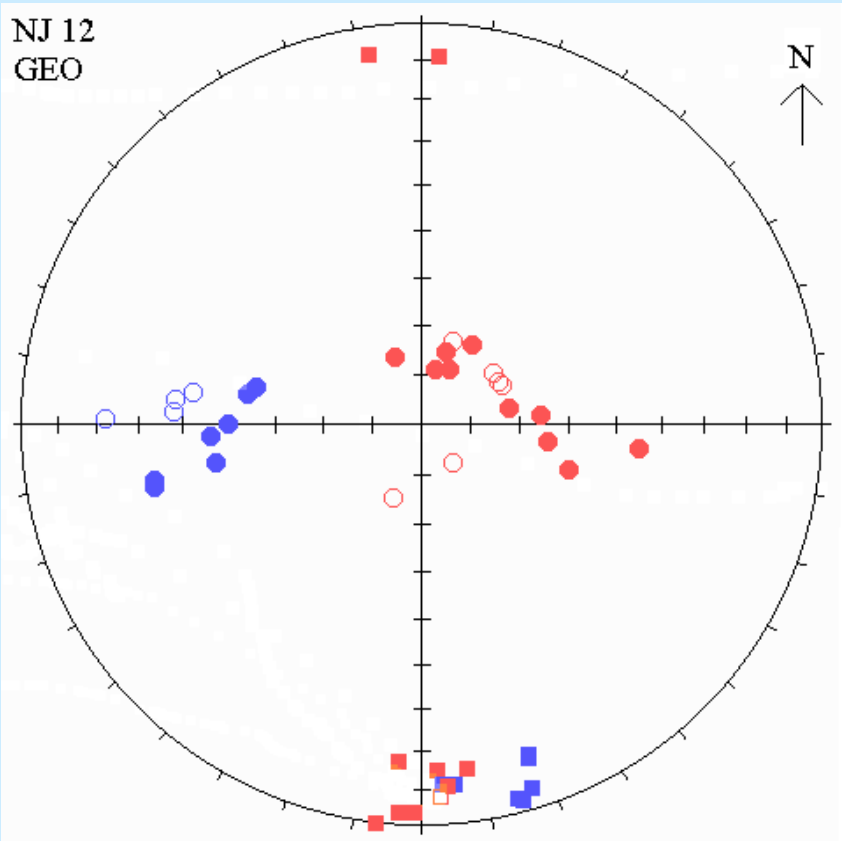
AMS IN FOLDS

Fold de-folding



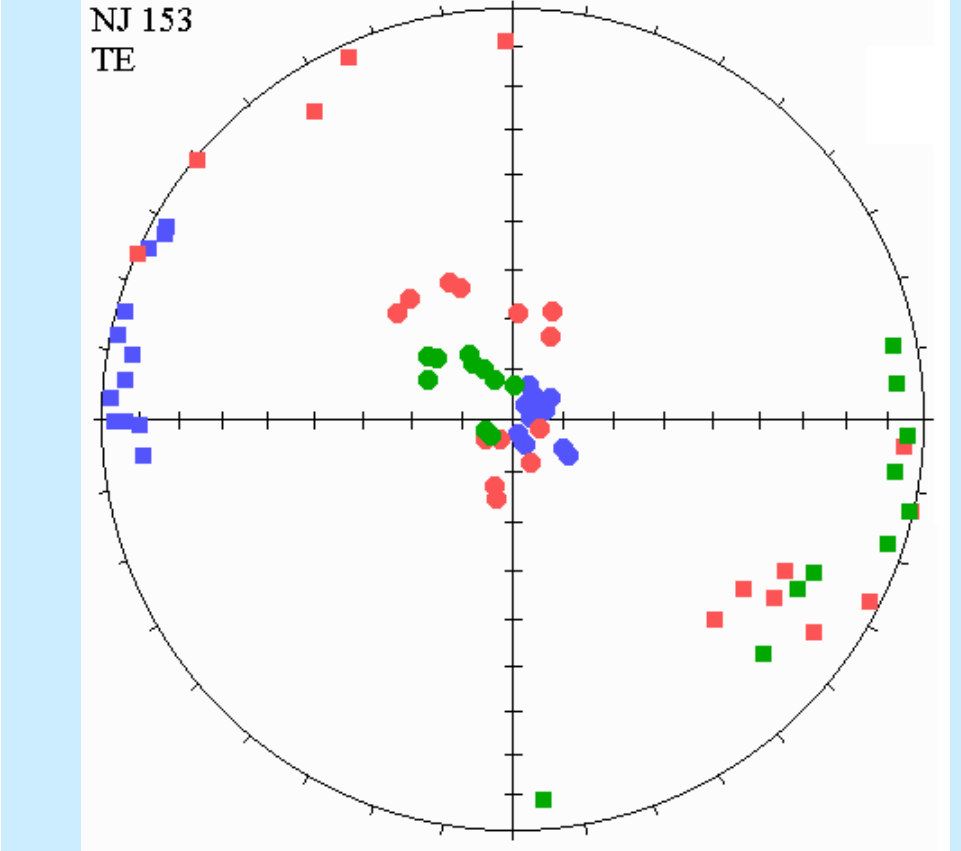
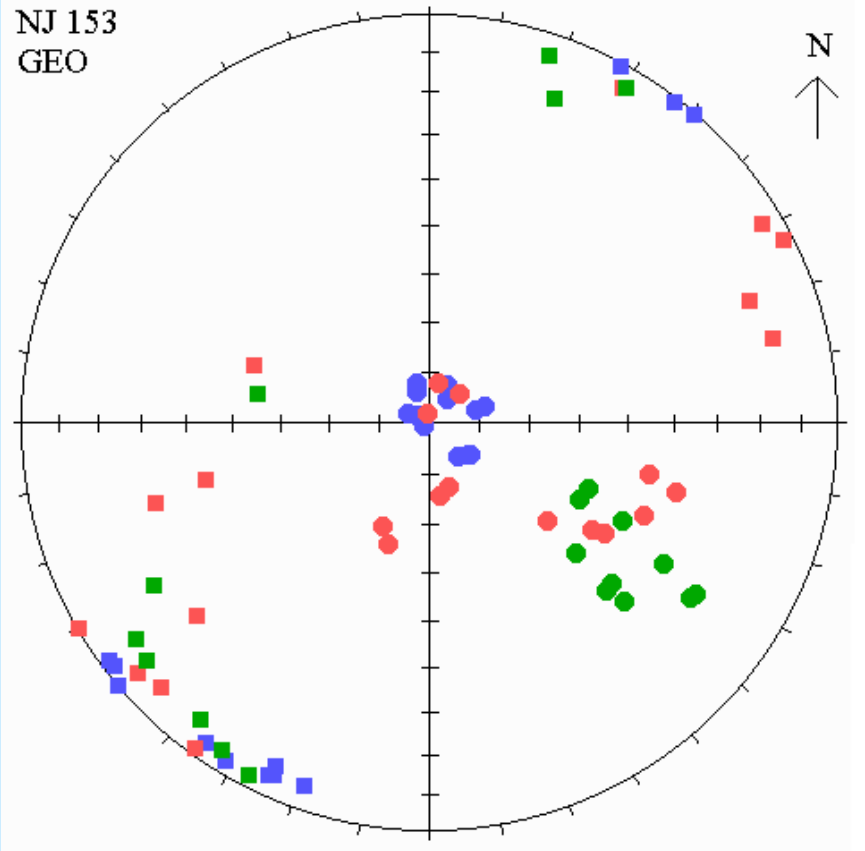
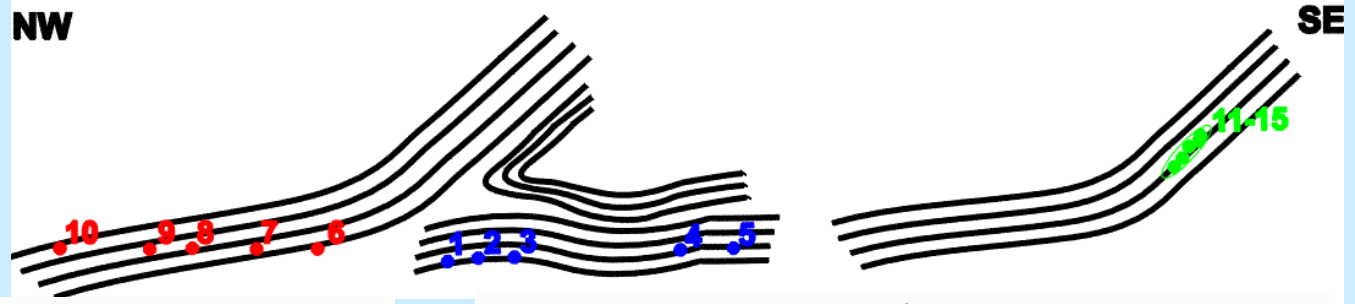
Obr. 80. a 81. Dílčí diagram D_1 (obr. 80, vlevo) a D_2 (obr. 81, vpravo) z vrásy ve vápenci od Velké Klajdovky. Orientace $\perp B$, v obou případech 200 os a hustota osazení $> 4-3-2-1-1\frac{1}{2}\%$. Podle J. Štelcila 1957, s. 440.

Buckle Fold NJ 12



NJ 153

Fold NJ 153-pd



Cleavage Fold NJ 23

